

1. Surface characteristics study in dry face milling of AZ91 alloy using PVD carbide inserts and optimization of process parameters using Grey Relational Analysis
Vikas Marakini, Srinivasa Pai P, Udaya Bhat K, Dinesh Singh Thakur & Bhaskara P. Achar 1
2. Development Of Alkali Activated Pervious Concrete Paver Blocks
Nidhishree, Shriram Marathe, I R Mithanthaya 8
3. A Review On Extraction, Purification And Structural Characterization of Plant Polysaccharides
Pannaga K N, Darshini S M and Vidya S M 15
4. Nasal Carriage of *Staphylococcus Aureus* Among Orphanage Children In and Around Mangalore
Dr. Radhakrishna M, Melreena Serra, Udayalaxmi J 21
5. Covid 19 Sentiment Analysis on Twitter Posts
Supreetha, Mangala 24

EDITORIAL



Like the Phoenix bird, the whole world has risen from ashes left behind by the Covid 19. The world is back again in full force. Having learned the lessons from the past mistakes it is time to put our best foot forward. In the aftermath of Covid, the world has arisen to see the emergence of artificial intelligence and machine learning in every walk of life; this, along with interest in the internet of things, has made life become one fabulous wonderland. Already in some advanced countries, the governments are trying out flying cars & robotic household help. These are made possible because of advancements in image processing, and the internet. In this issue of NMAMIT's annual research journal, every attempt has been made to cover advancements made in artificial intelligence, machine learning, and IoT. However other contemporary areas of Science and Management have been included. I request readers to contribute their research outputs to this journal in the coming years.

Happy Reading!

Dr. Sudesh Bekal

MEMBERS OF EDITORIAL BOARD

EDITOR-IN-CHIEF

Dr. Nirajjan N. Chiplunkar

NMAM Institute of Technology, Nitte

EDITOR

Dr. Sudesh Bekal

Dean (R&D),

NMAM Institute of Technology, Nitte

EDITORIAL BOARD

Dr. S. Y. Kulkarni

Professor & Additional Director,

B.N.M Institute of Technology, Bangalore

Dr. N. S. Sriram

Vidya Vikas College of Engineering, Mysore

Dr. Jaganath Nayak

National Institute of Technology Karnataka,

Suratkal

Dr. Shridhara S.

Indian Institute of Technology Bombay, Mumbai

Dr. Navakanth Bhat

Indian Institute of Science & Communication,

Bangalore

Dr. Gopalakrishna Kini

Manipal Institute of Technology, Manipal

EDITORIAL ASSISTANTS

Dr. Vasanth K R

Department of Mathematics

NMAMIT, Nitte.

Dr. Mangala Shetty.

Department of M CA,

NMAMIT, Nitte.

N.M.A.M.I.T.

Annual Research Journal

Volume 11

December 2021

ISSN 2249-0426

Published by:



**NMAM INSTITUTE
OF TECHNOLOGY**

N.M.A.M. INSTITUTE OF TECHNOLOGY

(An Autonomous Institution affiliated to VTU, Belagavi)
NITTE - 574 110, Karkala Taluk, Udupi District, Karnataka, India
www.nitte.edu.in/nmamit www.research.nitte.edu.in

Surface Characteristics study in dry face milling of AZ91 alloy using PVD carbide inserts and optimization of process parameters using Grey Relational Analysis

Vikas Marakini¹, Srinivasa Pai P*¹, Udaya Bhat K.², Dinesh Singh Thakur³ & Bhaskara P. Achar¹

¹Dept. of Mechanical Engineering, NMAM Institute of Technology, Nitte - 574110, India

²Dept. of Metallurgical and Materials Engineering, NITK, Surathkal -575 025, India

³Dept. of Mechanical Engineering., DIAT, Pune – 411 025, India

*Email: srinivasapai@nitte.edu.in

Abstract— High speed dry face milling is performed on AZ91 alloy using PVD coated carbide insert to study the material behaviour. Spindle speed, feed rate and depth of cut have been considered as inputs under high speed face milling. A Taguchi DOE statistical model is used to shorten the experimental time and cost and the outputs analysed are Surface Roughness and Hardness. Grey relational analysis method is implemented to identify the most optimal machining condition to achieve the most improved surface characteristics in terms of roughness and hardness. Further, statistical analysis such as Analysis of Variance and Signal to Noise ratio are also performed to identify the impact of input parameters affecting the surface characteristics. The study showed the effectiveness of Taguchi design combined with Grey Relational Analysis for the multi-objective problems such as surface characteristic studies.

Keywords—Face milling, roughness, hardness, Spindle speed, Feed rate, Depth of cut, Taguchi, Grey relational analysis.

I. INTRODUCTION

In the recent years, researchers have leaned towards magnesium alloys because of its remarkable qualities such as low density, high strength ratio, and high stiffness etc. Their other advantages include great recyclability and ease of machining [1,2]. Magnesium has a density of 1.7 g/cm³, makes it 30% lighter than aluminum and 75% lighter than steel [3]. They have several other appealing features such as good electrical and thermal conductivity [4]. Magnesium is found to be the second most abundant metal in seawater [5]. Magnesium and its alloys have both structural and non-structural aerospace applications [2,6]. When physical properties of magnesium are compared to those of other related elements, it is clear that magnesium outperforms them in major aspects [7]. Magnesium alloys' light weight aspects appeals to the aerospace and automotive industries in terms of efficient energy usage and reduced hazardous waste emissions [8]. According to general

data, the buy-to-fly ratio is frequently low (10-20%), indicating that approximately 80-90 percent of the material is scrapped during machining processes [9]. Among the magnesium alloys, AZ series alloys are one of the most well-known alloys in the market today [10]. In order to improve the operational performance of the components, a precise relationship between the machining parameters and the surface characteristics must be established. Milling is the most commonly used machining operation in the industry, and usually high speed milling is preferred to increase the productivity. Proper cutting parameter selection reduces the number of milling tests, resulting in cost savings.

II. MATERIALS AND EXPERIMENTAL DETAILS

A. Materials

AZ91 alloy block with size 50x50x50 mm is used in this study and its composition is shown in Table 1. The milling cutter SECO R220.69-0050-12-5AN) and the PVD coated carbide inserts (SECO XOEX10T304FR-E05 F40M) with rake angle of 21.6° are used (Fig. 1 & Fig. 2).

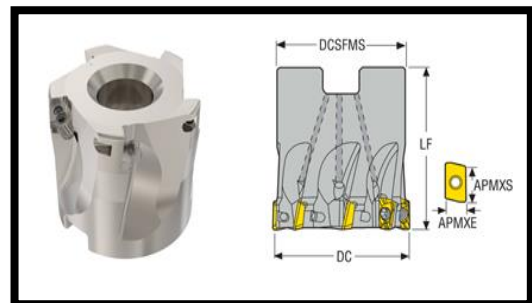


Fig. 1 Cutter geometry

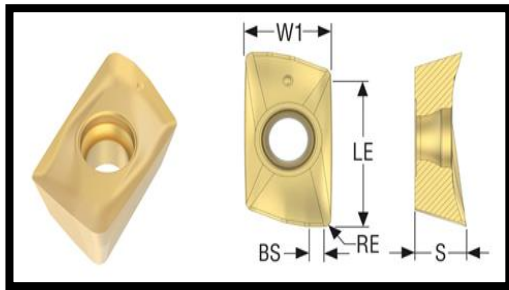


Fig. 2 Insert geometry

TABLE 1
MATERIAL COMPOSITION

Element %						
Al	Zn	Mn	Cd	Cu	Ni	Mg
9.12	0.98	0.47	0.00	0.00	0.00	89.43

B. Experimental details

The range of cutting parameters selected for the present study are listed in Table 2. Experimental conditions selected from the Taguchi L9 design of experiments (DOE) model using MINITAB 17 software are listed in Table 3. This type of model reduces the cost and time associated with the project, by reducing the number of experiments. CNC Milling Machine (BMV 45 T20) which has the capacity of 6000 RPM spindle speed is used for experimental work (Fig. 3). Machining experiments are performed for fixed 50 mm cutting length and new insert is used for each experiment to avoid the effect of possible wear. After each machining pass, the surface roughness (Ra) is obtained using TalySurf 50 (Taylor Hobson) device as shown in Fig. 4. Nine readings of Ra are measured for each machining pass and the resultant mean Ra values are shown in Fig. 6. Similarly, surface microhardness (HV) after each machining pass is obtained using Vickers Microhardness HM-200 (Mitutoyo) device as shown in Fig. 5. For testing, load used was 50 gf for the duration of 10 seconds. Nine readings of HV are measured for each machined surface and the resultant mean HV are shown in Fig. 7. Surface roughness and microhardness of the Base Material (BM) are observed to be 0.44 μm and 69 HV respectively.



Fig. 3 Face milling setup



Fig. 4 Surface roughness test



Fig. 5 Vickers hardness test

TABLE 2
MACHINING PARAMETERS

Parameter	Level 1	Level 2	Level 3
Spindle speed V m/min	500	700	900
Feed rate/teeth f mm/z	0.1	0.2	0.3
Depth of cut a mm	0.5	1.0	1.5

TABLE 3
TAGUCHI DESIGN

Exp. No.	Spindle speed	Feed rate	Depth of cut
1	500	0.1	0.5
2	500	0.2	1
3	500	0.3	1.5
4	700	0.1	1
5	700	0.2	1.5
6	700	0.3	0.5
7	900	0.1	1.5
8	900	0.2	0.5
9	900	0.3	1

III. RESULTS

A. Experimental results

The mean results of surface roughness and microhardness are shown in Fig. 6 and Fig. 7 respectively. A comparison between the base material and the machined surfaces clearly showed a significant improvement in both surface roughness and microhardness, which can be seen in Fig. 6 and Fig. 7 respectively. Surface roughness and hardness are important factors in the study of material surface integrity due to their relation with corrosion and wear resistance. The impact of surface roughness on improving the material corrosion properties have been discussed elsewhere [11–12]. Improving the surface hardness on improving the surface integrity of the material in terms of wear and corrosion resistance is well discussed elsewhere [13–14]. To summarize, smoother and harder the surface better is the wear and corrosion resistance of the material.

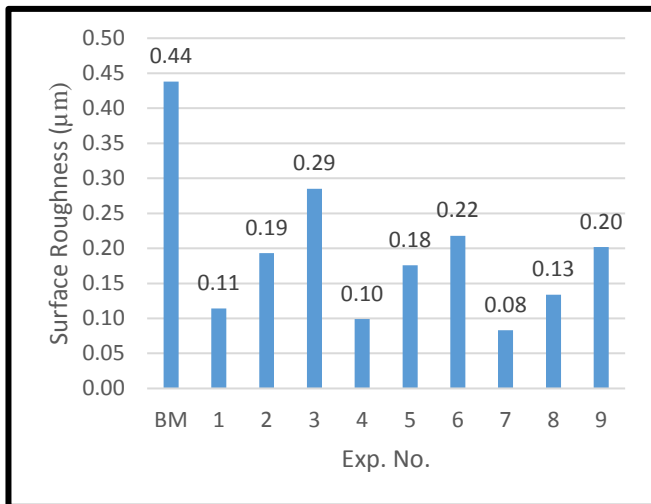


Fig. 6 Surface Roughness values (Ra)

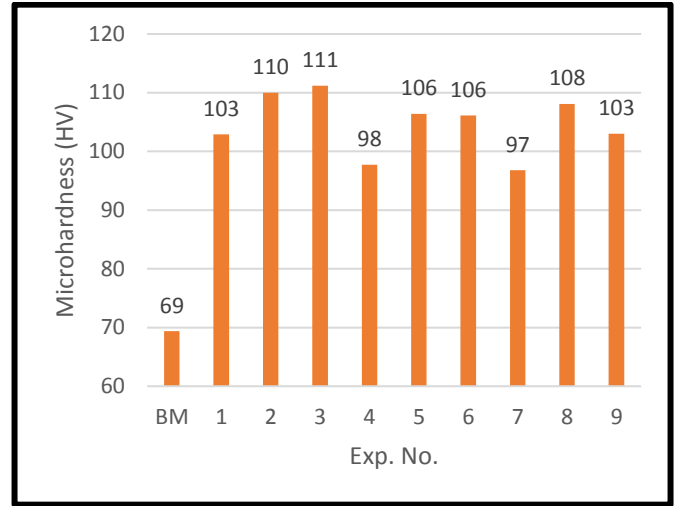


Fig. 7 Microhardness values (HV)

B. Optimization

Grey Relational Analysis (GRA) is a decision making tool which converts multiple objectives into a single objective [15]. Present study focusses on identifying the most optimal condition considering the requirements such as lower the better surface roughness and higher the better microhardness. Therefore, GRA is identified as the most suitable method for the present study. GRA is performed using the following steps:

a) *Normalizing*: The normalization step involves using lower the better or higher the better characteristics. In the present study, lower the better is the requirement for surface roughness and higher the better is the requirement for microhardness. Equations are as follows -

‘Lower the better’ equation:

$$y_i^*(k) = \left(\frac{\max x_i^0(k) - x_i^0(k)}{\max x_i^0(k) - \min x_i^0(k)} \right) \quad (1)$$

‘Higher the better’ equation:

$$y_i^*(k) = \left(\frac{x_i^0(k) - \min x_i^0(k)}{\max x_i^0(k) - \min x_i^0(k)} \right) \quad (2)$$

Here, $x_i^0(k)$ = measured values,

$\max x_i^0(k)$ = maximum value of $x_i^0(k)$ values,

$\min x_i^0(k)$ = minimum of $x_i^0(k)$ values,

i = number of tests, k = quality characteristic.

b) *Grey relational coefficient (GRC)*: It is evaluated using the equation -

$$\epsilon_i(k) = \left(\frac{\Delta_{\min} - \zeta \Delta_{\max}}{\Delta_{0i}(k) - \zeta \Delta_{\max}} \right) \quad (3)$$

Here, $\Delta_{0i}(k)$ = Offset absolute values between $y_0^*(k)$ & $y_i^*(k)$,
 $\zeta = 0.5$ = distinguishing coefficient,
 Δ_{\min} and Δ_{\max} = least and highest of $\Delta_{0i}(k)$.

c) Grey relational grade (GRG): It is evaluated by averaging the value of GRG using the equation -

$$\gamma_i = \frac{1}{n} \sum_{k=1}^n \epsilon_i(k) \quad (4)$$

Here, γ_i varies between 0 to 1,
 n = number of tests.

TABLE 4
GREY RELATIONAL ANALYSIS

EXP. NO.	Ra	HV	Ra	HV	Ra	HV	GRG	RANK
	NORMALIZED	DEV. SEQ.	GRC					
1	0.847	0.424	0.153	0.576	0.765	0.465	0.615	5
2	0.455	0.917	0.545	0.083	0.479	0.857	0.668	2
3	0.000	1.000	1.000	0.000	0.333	1.000	0.667	3
4	0.921	0.063	0.079	0.938	0.863	0.348	0.606	6
5	0.540	0.667	0.460	0.333	0.521	0.600	0.560	7
6	0.332	0.646	0.668	0.354	0.428	0.585	0.507	8
7	1.000	0.000	0.000	1.000	1.000	0.333	0.667	3
8	0.748	0.785	0.252	0.215	0.664	0.699	0.682	1
9	0.411	0.431	0.589	0.569	0.459	0.468	0.463	9

GRA implemented values for surface roughness and microhardness, using equations (1), (2), (3) and (4) are listed in Table 4. Calculations and analysis of GRA is performed using MS Excel 2016 software. Corresponding ranks based on the largest GRG value to the smallest is also listed in Table 4. From this analysis, it is evident that the highest GRG value represents the most optimal condition for improved surface integrity of the selected material in terms of surface roughness and microhardness. Therefore, the most optimal condition is identified as A3B2C1(Rank 1): $V=900$ m/min, $f=0.2$ mm/teeth, & $a=0.5$ mm.

C. Discussions

Statistical tools such as ANOVA and Signal-to-Noise ratio (S/N) uses estimation procedures which are normally used to make conclusions in problems involving reduced number of experiments. Their application in surface integrity studies can also be seen in [15-16]. ANOVA and S/N ratio analysis are

performed for surface roughness, microhardness and GRG's using MINITAB 17 statistical software [17-18].

TABLE 5
RESPONSE TABLE – SURFACE ROUGHNESS

Smaller is better			
Level	Spindle Speed V	Feed Rate f	Depth of Cut a
1	14.68	20.19	16.52
2	16.14	15.61	16.09
3	17.66	12.68	15.87
Delta	2.97	7.51	0.65
Rank	2	1	3

TABLE 6
ANOVA – SURFACE ROUGHNESS

Factors	DOF	SS	MS	Contribution (%)
Spindle speed	2	13.25	13.25	13.22
Feed rate	2	86.02	86.02	85.85
Depth of cut	2	0.64	0.64	0.64
Error	2	0.28	0.28	

Surface roughness is found to be most influenced by feed rate as can be seen from the values of Table 5. Similar observation is also reported in [13,19]. The ANOVA results of the present study on surface roughness is presented in Table 6. The contribution of feed rate, spindle speed & depth of cut on surface roughness is 85.85 %, 13.22 % and 0.64 % respectively. Further, Taguchi mean plot for surface roughness is shown in Fig. 8. The most notable observation is the increase in surface roughness with increase in feed rate, which may have been due to the increase in material removal rate. Feed rate increase leads to an increase in friction at the tool-workpiece contact area resulting in high surface roughness [20-21]. Further, from Fig. 9 the optimum conditions for lowest surface roughness is A3B1C2: $V=900$ m/min, $f=0.1$ mm/teeth, & $a=1.0$ mm.

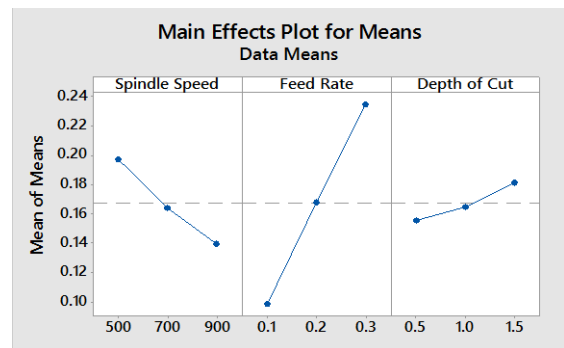


Fig. 8 Effect of machining parameters on Roughness

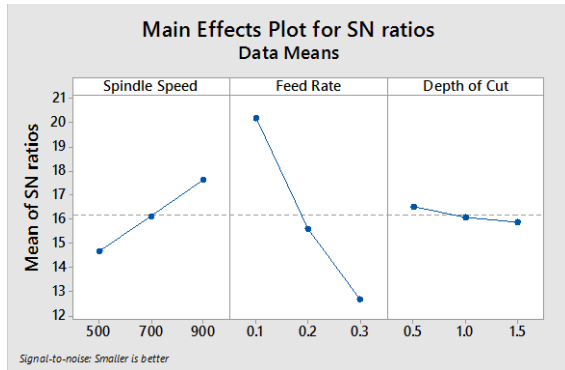


Fig. 9 Predicted optimal condition for Roughness

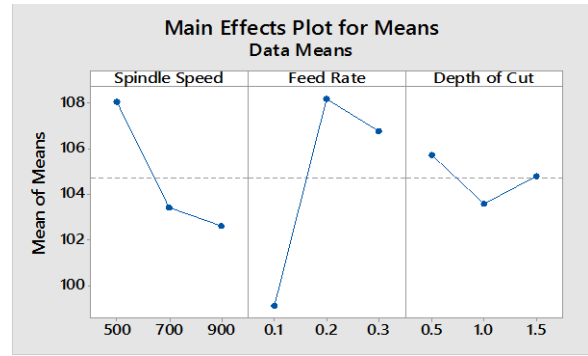


Fig. 10 Effect of machining parameters on Microhardness

For microhardness, the most dominant factor is observed to be the feed rate (Table 7). Among the findings from previous researchers, there has been evidence of feed rate having significant influence on microhardness [13]. The ANOVA results of the present study on microhardness is presented in Table 8. The contribution of feed rate, spindle speed & depth of cut on microhardness is 69.67 %, 24.55 % and 3.60 % respectively. Further, Taguchi mean plot for microhardness is shown in Fig. 10. Here, the most notable observation is the decrease in hardness with increase in spindle speed, which may have been due to the rise in temperature. Spindle speed increase leads to increase in temperature at the tool-workpiece contact area resulting in thermal softening [22-23]. Further, from Fig. 11 the optimum conditions for highest microhardness is A1B2C1: $V=500$ m/min, $f=0.2$ mm/teeth, & $a=0.5$ mm.

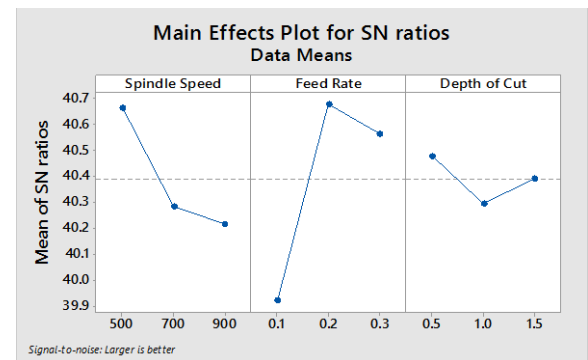


Fig. 11 Predicted optimal condition for Microhardness

TABLE 7
RESPONSE TABLE – MICROHARDNESS

Larger is better			
Level	Spindle Speed V	Feed Rate f	Depth of Cut a
1	40.67	39.92	40.48
2	40.28	40.68	40.29
3	40.22	40.46	40.39
Delta	0.45	0.76	0.19
Rank	2	1	3

TABLE 8
ANOVA – MICROHARDNESS

Factors	DOF	SS	MS	Contribution (%)
Spindle speed	2	0.35	0.35	24.55
Feed rate	2	1.00	1.00	69.67
Depth of cut	2	0.05	0.05	3.60
Error	2	0.02	.02	

The impact of the type of inserts used for face milling operation on the work material surface characteristics is also observed by comparing the findings of the present study (PVD coated carbide insert) with our previous study (Uncoated carbide insert) [24], which is presented in Table 9. Comparison showed some similarities in the behaviour of cutting parameters such as feed rate on surface roughness and spindle speed on microhardness. Comparison also showed similarity in terms of the most optimal conditions with slight changes in GRA rankings between them. A major observation is the significant difference in the improvement of microhardness from machining using PVD insert when compared to the Uncoated insert. Further tests such as microstructure and residual stresses are required to differentiate these two inserts in terms of their impact on the overall surface integrity characteristics of the alloy, which will be covered in the future publications.

TABLE 9
COMPARISON OF INSERTS FOR MACHINING

PVD coated carbide	Uncoated carbide
<ul style="list-style-type: none"> Surface roughness improvement of upto 81% from the RAW material. 	<ul style="list-style-type: none"> Surface roughness improvement of upto 85% from the RAW material.

<ul style="list-style-type: none"> Microhardness improvement of upto 60% from the RAW material. 	<ul style="list-style-type: none"> Microhardness improvement of upto 33% from the RAW material.
<ul style="list-style-type: none"> Surface roughness values increased with increase in feed rate. 	<ul style="list-style-type: none"> Surface roughness values increased with increase in feed rate.
<ul style="list-style-type: none"> Microhardness values decreased with increase in spindle speed. 	<ul style="list-style-type: none"> Microhardness values decreased with increase in spindle speed.
<ul style="list-style-type: none"> GRA Rank: 1. A3B2C1 (Exp. No. 8) 2. A1B2C2 (Exp. No. 2) 3. A3B1C3 (Exp. No. 7) 	<ul style="list-style-type: none"> GRA Rank: 1. A1B2C2 (Exp. No. 2) 2. A3B1C3 (Exp. No. 7) 3. A3B2C1 (Exp. No. 8)

IV. CONCLUSIONS

In this work, high speed dry face milling is performed on AZ91 magnesium alloy using PVD coated carbide inserts. Surface characteristics such as roughness and hardness are measured for a set of experiments selected from taguchi design of experiments. Further, statistical analysis is performed and the conclusions are listed as follows:

- High speed machining resulted in great improvement in surface roughness and surface hardness of the alloy. Lowest roughness value is observed to be 81% improvement from the RAW material. Highest hardness value is observed to be 60% improvement from the RAW material.
- With regard to the cutting parameters of the present study, surface roughness shows improvement for lower feed rate and microhardness shows improvement for lower spindle speed. The optimum conditions for lowest surface roughness is A3B1C2: $V=900$ m/min, $f=0.1$ mm/teeth, & $a=1.0$ mm and the optimum conditions for highest microhardness is A1B2C1: $V=500$ m/min, $f=0.2$ mm/teeth, & $a=0.5$ mm.
- GRA successfully identified the most optimal condition for combined multiple characteristics. The most optimum condition: A3B2C1 (Rank 1): $V=900$ m/min, $f=0.2$ mm/teeth, & $a=0.5$ mm is a high speed condition, which encourages the application of high speed milling for improving the surface integrity of the alloy.

ACKNOWLEDGMENT

The authors thank the Aeronautics R & D Board, DRDO, New Delhi for the funding support. Sanction Code: MSRB/TM/ARDB/GIA/19-20/044.

REFERENCES

- B. L. Mordike., & T Ebert.. Magnesium. *Materials Science and Engineering: A*, 2001, 302(1), 37–45.
- S Pai., & B Achar. “machining of magnesium alloys: a review”. *Manufacturing Technology Today*, 2017, 16(08), 10–23.
- I Ostrovsky. & Y Henn. Present state and future of magnesium application in Aerospace industry. ‘*ASTEC’07 International Conference - New Challenges in Aeronautics*, 2007, Moscow, 1-5.
- D Carou, & P J Davim, *Machining of Light Alloys* (1st ed.), 2021, CRC Press.
- J Jayaraja, M Prasanth, A Srinivasan, U Pillai. & B Pai. Magnesium – in Indian Context. ‘*Indian Foundry Journal*’, 2015, 61(2), 49-55.
- M Kutz. *Mechanical Engineers’ Handbook*, Volume 1: Materials and Mechanical Design (3rd ed., Vol. 1). Wiley, 2005.
- H Watara. Trend of Research and Development for Magnesium Alloys - Reducing the Weight of Structural Materials in Motor Vehicles. *SCIENCE & TECHNOLOGY TRENDS*, 2006, 7, 84-97.
- B Akyüz. Comparison of the machinability and wear properties of magnesium alloys. *The International Journal Of Advanced Manufacturing Technology*, 2014, 75(9-12), 1735-1742.
- A Angrish. A critical analysis of additive manufacturing technologies for aerospace applications, *2014 IEEE Aerospace Conference*, 2016, 1-6.
- Wikipedia contributors. *Magnesium alloy*, Wikipedia, 2021.
- A Samaniego., I Iorente., & S Feliu.. Combined effect of composition and surface condition on corrosion behaviour of magnesium alloys AZ31 and AZ61, *Corrosion Science*, 2013, 68, 66–71.
- U Reddy, D Dubey, S S Panda, I reddy, J Jain, Mondal, K., & S S Singh, Effect of Surface Roughness Induced by Milling Operation on the Corrosion Behavior of Magnesium Alloys, *Journal of Materials Engineering and Performance*, 2021.
- K Shi., D Zhang, J Ren, C Yao, & X Huang. Effect of cutting parameters on machinability characteristics in milling of magnesium alloy with carbide tool, *Advances in Mechanical Engineering*, 2016, 8(1).
- M Danish., Raubaiee, S. & H Ijaz.. Predictive Modelling and Multi-Objective Optimization of Surface Integrity Parameters in Sustainable Machining Processes of Magnesium Alloy. *Materials*, 2021, 14(13), 3547.
- K Shi, D Zhang. & J Ren.. Optimization of process parameters for surface roughness and microhardness in dry milling of magnesium alloy using Taguchi with grey relational analysis. *The International Journal of Advanced Manufacturing Technology*, 2015, 81, (1–4), 645–651.
- B Eker. B Ekici, M Kurt. & B Bakir. Sustainable machining of the magnesium alloy materials in the CNC lathe machine and optimization of the cutting conditions. *Mechanics*, 2014, 20(3).
- M S Ruslan, K Othman, A. Ghani, J., Kassim, M.S. & CheHaron, C.H.. Surface roughness of magnesium alloy AZ91D in high speed milling. *Journal Teknologi*, 2016, 78(6-9).

18. S Ramesh, R Vishwanathan. & S Ambika.. Measurement and optimization of surface roughness and tool wear via grey relational analysis, TOPSIS and RSA techniques. *Measurement*, 2016, 78, 63-72.
19. I Zagorski., & J Korpysa. Surface Quality Assessment after Milling AZ91D Magnesium Alloy Using PCD Tool. *Materials*, 2020, 13(3), 617.
20. S Dinesh., V Senthilkumar, P Asokan., & D Arulkirubakaran, Effect of cryogenic cooling on machinability and surface quality of bio-degradable ZK60 Mg alloy. *Materials & Design*, 2015, 87, 1030-1036.
21. M Danish, T L Ginta., A M Abdul Rani, D Carou, D, J Davim, Rubaiee, S. & Ghazali, S.. Investigation of surface integrity induced on AZ31C magnesium alloy turned under cryogenic and dry conditions. *Procedia Manufacturing*, 2019, 41, 476-483.
22. M Danish, T L Ginta, K Habib, D Carou, AM A Rani, & B B Saha. Thermal analysis during turning of AZ31 magnesium alloy under dry and cryogenic conditions. *The International Journal of Advanced Manufacturing Technology*, 2017, 91(5-8).
23. M Danish., T L Ginta. K Habib., A M Abdul Rani, & B B Saha., Effect of Cryogenic Cooling on the Heat Transfer during Turning of AZ31C Magnesium Alloy. *Heat Transfer Engineering*, 2018, 40(12), 1023-1032.
24. V Marakini., S Pai, U Bhat, D Thakur. & B Achar.. High speed machining for enhancing the AZ91 Magnesium alloy surface characteristics: influence and optimization of machining parameters. Accepted for publication in *Defense Science Journal*, 2021.

Development of Alkali Activated Pervious Concrete Paver Blocks

Nidhishree¹, Shriram Marathe*², I R Mithanthaya³

Department of Civil Engineering
NMAM Institute of Technology, Nitte, India

¹nidhi8996shree@gmail.com

³irmithanthaya@nitte.edu.in

*Corresponding Author

²shrirammarathe@nitte.edu.in

Abstract— Concrete is one of the vastly used building materials on earth. In traditional concrete, Portland cement is used. Portland cement manufacture entails the large-scale exploitation of natural reserves of limestone, clay, and coal. As a result, there is a need for supplementary construction material development, such as Fly-ash, Ground Granulated Blast Furnace Slag (GGBS), and other industrial by-products. Alkali Activated Concrete is an advanced and eco-friendly construction material that incorporates Fly Ash or GGBS, and Sodium Hydroxide or Potassium Hydroxide, Sodium Silicate, or Potassium Silicate, as alkali activators which avoids the necessity of Portland cement. We have utilized alkali-activated concrete to manufacture pervious concrete paver blocks in this study. Water management can be done easily with pervious paver blocks. They work by providing a solid surface while also enabling water to freely drain into the earth through the voids. Several stormwater treatment issues can be solved in this manner. the research aims to develop sustainable pervious concrete paver blocks to utilize them as pavement For this purpose, numerous mixes with different proportions of these industrial wastes were cast as per Indian standards. Voids were created according to the fabrication details.

Keywords— concrete, alkali-activated, pervious, blocks.

I. INTRODUCTION

Concrete is one of the most extensively utilized building materials on earth. After water, concrete is the next widely used material. The manufacture of Portland cement entails the large-scale exploitation of natural limestone, clay, and coal reserves. According to estimates, the manufacture of one ton of Portland cement will release 0.9 tons of carbon dioxide into the atmosphere. Given this, ancillary construction materials based on industrial by-products such as Ground Granulated Blast Furnace Slag (GGBS), fly ash which is high in alumina, and silica, are essential to reduce the carbon footprint of concrete[1][2]. Alkali Activated Concrete is a pioneering and environmentally friendly construction material that uses Fly Ash or GGBS, alkali activators like Potassium

Hydroxide or Sodium Hydroxide, Potassium Silicate or Sodium Silicate, and reduces the necessity of Portland cement. The remaining mixture is made of Ordinary coarse and fine aggregates, as well as water, which is added to enhance workability. The ingredients can be mixed with low alkali materials and cured in a short amount of time in natural conditions. Retaining walls, Pavements, water-tanks, precast bridge decks, and other structures can be constructed with this [3]. As hard surfaces are built using concrete, it leads to surface runoff, which can result in, pollution, flooding, and soil erosion. Pervious concrete is a distinct type of high-porosity concrete used for flatwork applications that allows water from precipitation and other sources to penetrate directly, decreasing runoff and permitting groundwater recharging. The high porosity is achieved through a highly interconnected void content. Pervious concrete is made with a high void content (15-25%) and water to cement ratio of 0.35 to 0.45. Pervious concrete pavements help to reduce the urban heat island effect in addition to stormwater control. Unlike a standard asphalt surface, pervious concrete pavements do not collect and retain heat before radiating it back into the environment[4]. One of the most prevalent flexible surface treatment solutions for external pavement applications is paver block or paver block. These blocks are attractive, comfortable to walk on, long-lasting, and simple to maintain. They come in a variety of shapes, sizes, colors, textures, and patterns[5]. The current study aims to design and develop the alkali-activated pervious paver blocks and to study the strength of the blocks.

II. LITERATURE REVIEW

Chandrappa and Biligiri (2018): in this journal, efforts are made to evaluate the flexural strength and stiffness of pervious concrete. the ingredients used for the preparation of the concrete were a coarse aggregate of calcareous and crushed type. the four aggregate sizes were used for the proportioning the gradation that included 19-13.2mm,13.2-

9.5mm, 9.5-6.7mm, and 6.7-4.75mm. the 20 mm down size aggregate were having 2.872 specific gravity and 1.34% of water absorption. Two single-sized gradations were having 9.5mm -6.7mm and 13.2mm -9.5mm aggregates and were named as P₂ and P₃. the binary gradation comprised of 50% 6.7-4.75mm and 50% 9.5-6.7mm and were named as P₄. the ternary gradation comprised of 25% of 19-13.2mm and 25% 13.2-9.5mm and 25% 9.5-6.7mm and 25% 6.7-4.75mm. the two-level of water-cement ratio was selected 0.3 and 0.35 and three levels of cement to aggregate ratio were selected that is 0.2, 0.25, and 0.33, ordinary Portland cement (OPC) of 53 grade were selected, lingo sulfate-based plasticizer was used to improve the workability of concrete. depending on the various combination of gradations, water to binder ratio, and cement to aggregate ratio, 15 concrete mixtures were prepared. the beam specimen of 500X100X100mm size were prepared and cured in water for 28 days. and the four-point bending beam test was carried out. The flexural strength of pervious concrete varied from 1.5-3.3 MPa [6].

Hassan and Kianmehr (2018): in this journal the study is carried out on the pervious concrete by incorporating the GGBS. The materials used for the preparation of the concrete were OPC type 1, 20mm and 10mm aggregates and Anti-fire crack and Asota micro-crack preventer 18 fibers. A total of 11 types of the concrete mixture were prepared by varying aggregate contents, fiber content, and porosity. W/C selected was 0.3 and cement was replaced up to 50% by GGBS. 0.6kg of 18 mm polypropylene were incorporated into the concrete mixture. The specimens prepared were cured for 7 and 28 days and subjected to tensile strength and compressive strength tests. The compressive strength of 54MPa was obtained for the 28 days of curing for the concrete mixture with 20mm aggregate and 10% of porosity and 0.6 kg of polypropylene fibers and concrete mixture with ordinary Portland cement and 10mm aggregate and 10% porosity attained the highest split tensile strength of 5MPa [7].

Hesami et al (2014): in this journal, the investigation is carried out on the pervious concrete by using rice husk and fiber. the constituents used for the preparation of the pervious concrete were a coarse aggregate of size 2.36-19mm, Portland cement type II, rice husk ash, carboxylic ether superplasticizer, glass fibers, steel fibers, and polypropylene sulfide fibers. 104 types of the concrete mixture were prepared namely A, B, C and D. the mix A, B, C were having the water to cement ratio (W/C) of 0.27, 0.33 & 0.4 and 0.5% steel, 0.2% glass, and 0.3% PPS fibers, and the cement content was replaced by 0%, 2%, 4%, 6%, 8%, 10% and 12% of rice husk ash in each mix. the concrete mixture D was prepared using 4, 8, & 12% of rice husk ash and without fibers. the beam specimen of size 100X100X500mm were prepared and cured in water for 28 days and subjected to a flexural strength test the concrete mix with polypropylene fiber with W/C of 0.33 showed the highest flexural strength of 2.8 MPa. concrete mix with 10% rice husk ash and with steel fiber showed the highest flexural strength of 4.2 MPa [8].

Muthukumar et.al (2020): in this journal the experimental investigation was carried on the eco-friendly pervious concrete and its mechanical properties. the ingredients used for the preparation of the concrete OPC of 53 grade having a specific gravity of 2.98, aggregates of various sizes like 10mm, 12.5mm, 16mm, and 20mm sugarcane bagasse ash. the 6 types of concrete mixes were prepared by substituting cement with sugarcane bagasse ash at different percentages like 0%, 5%, 10%, 15%, 20%, and concrete specimens of size 100mmX100mmX500mm were cured in water for 7 and 28 days and subjected to flexural strength test and maximum flexural strength of 3.4 MPa was obtained for the 15% of sugarcane bagasse ash [9].

Palankar and Mithun (2018): In this literature experimental investigation is carried out by replacing Coarse aggregate with the steel slag aggregate in alkali-activated concrete for the application of concrete pavement. Here the natural CA is replaced 0%, 25%, 50%, 75%, 100% by volume using steel slag aggregate. The workability of Alkali Activated Slag/Flyash Concrete (AASFC) mixture with steel slag is slightly lowered with the increase in the steel slag content. The obtained slump values for 0%, 25%, 50%, 75%, 100% replacement of steel slag is 60mm, 55mm, 45mm, 40mm, 30mm respectively. The compressive strength test is carried out 3, 7, 28, 90 days of curing. Strength gain in early days is higher with replaced concrete than ordinary concrete conventional aggregate has a lower density than the steel slag. A flexural strength test was carried out after 7, 28, 90 days of curing. split tensile strength and Modulus of elasticity test was carried out for 28 days. for 0% replacement, it is noted that M.E is slightly lower than OPCC. AASFC exhibits better fatigue life than OPCC. As the stress level decreases from 0.85-0.70 there will be an increase in the fatigue life of the concrete specimen [10].

Marathe et.al (2021): In this paper detailed a study was carried out on the performance evaluation of alkali-activated concrete. The Materials used for the concrete preparation are GGBS, Fly-ash, powdered waste glass, stone crusher dust, crushed granite aggregate, alkaline activator. The compressive strength test result for various % of glass powder (0-25%) for 15% dosage maximum compressive strength of 68 MPa was achieved for 28 days. Further, the optimum flexural strength of 5.94 MPa was achieved for the AAC mix with a 15% dosage of glass powder [4].

III. EXPERIMENTS

A. Objective:

The core objective of the study is to develop, alkali-activated pervious concrete paver blocks To achieve the same, the following objectives have been set.

- 1) To develop the pervious paver block fabrications.
- 2) To design the Alkali activated concrete mix proportion of pervious paver blocks to achieve target performance.

Development Of Alkali Activated Pervious Concrete Paver Blocks

- 3) To investigate the mechanical strength of alkali-activated concrete pervious paver blocks.

B. Methodology:

- 1) Preliminary tests on materials i.e specific gravity, sieve analysis, water absorption test are conducted.
- 2) Preparation of CAD drawings of paver blocks elements.
- 3) Fabrication of pervious paver blocks elements.
- 4) Mix Design of Alkali Activated Concrete as per Indian standards.
- 5) Evaluation of mechanical properties by conducting laboratory tests.

C. Materials Used:

1) *Coarse Aggregate:* Locally accessible crushed granite stone aggregate with a maximum size of 10 mm was used. The coarse aggregate passing through a 10 mm sieve and retaining a 4.75mm sieve was used for experimental work. The properties of coarse aggregates were decided as per IS: 2386- 1963 and mentioned in Table 1.

TABLE I
PROPERTIES OF COARSE AGGREGATE

Sl.no	Properties	Test results
1	Specific gravity	2.62
2	Fineness modulus	2.4
3	Water absorption	Nil

2) *Fine Aggregate:* The locally accessible river sand, passing through a 4.75 mm sieve and retaining in 150 microns sieve used this

Sl.no	Properties	Test results
1	Specific gravity	2.64
2	Fineness modulus	7.5
3	Water absorption	1%

experimental work. The properties of fine aggregates were decided as per IS: 2386-1963[16] and are shown in Table 2.

TABLE II
PROPERTIES OF FINE AGGREGATE

3) *Fly ash:* Fly ash mainly comprises silt-sized particles which are spherical, and the size ranges from 10 to 100 microns. The fluidity and workability of fresh concrete can be improved using These small glass spheres. Fineness contributes to the pozzolanic reactivity of fly ash. The Specific Gravity of Fly Ash is 2.16.



Fig .1 Fly Ash

4) *Ground Granulated Blast Furnace Slag:* Blast-furnaces function at the temperature of about 1,500°C and are fed with a precisely controlled mixture of coke, limestone, and iron ore. The iron ore is condensed to iron and the remaining materials form a slag. Due to the decrease in heat of hydration, the increase in the temperature will be less avoiding the risk of thermal cracking. High resistance to chloride attack decreases the risk of corrosion in concrete.



Fig.2 GGBS

5) *Sodium Silicate (Na₂SiO₃):* Sodium silicate has found numerous uses in cementitious materials. For example, it is imposed as an alkali-activator in alkali-activated cement. In concrete, it is utilized as a setting accelerator. It is also familiar as water-glass or liquid glass; these materials are accessible in aqueous solution and solid form. The original compositions are colorless or white, but in the market pale low or light lime color in appearance can be seen due to some impurities.

6) *Caustic Soda Flakes (NaOH):* Caustic soda flakes are technically known as sodium hydroxide flakes. flake masses are of white color, hygroscopic, soluble in alcohol and water. The formula is NaOH. Technically sodium hydroxide flakes are produced by evaporating liquid caustic soda A grade. NaOH is bitter and has a soapy feel to it. Sodium hydroxide is strongly alkaline.

7) *Water:* comprising less than 2000 parts per million (ppm) of total dissolved solids can be utilized for the making of concrete. Water comprising more than 2000 ppm of dissolved solids must be tested for its effect on setting time

Development Of Alkali Activated Pervious Concrete Paver Blocks

and strength. PH of water to even 9 is allowed. As local water is saline and have no alternate sources, the chloride concentration up to 1000 ppm is even permitted for drinking. But this high amount of alkali carbonates and bicarbonates, in some natural mineral water, may cause an alkali-silica reaction. For this project, potable water according to IS: 456-2000 has been used.

8) *Alkaline Solution:* The mixture of Sodium silicate and Soda Flakes was used to prepare the alkaline solution. The Sodium silicate had a purity of 96-97% in the form of a solution and Soda (NaOH), in flake or pellet form, was used. The solids have to be dissolved in water to make a solution with the required concentration.



Fig .3 Alkaline solution

9) *Mild Steel Cover Pate:* Let A simple metal plate made up of mild steel (MS) of 10 mm thickness whose one side consists of mild steel metal spikes of diameter 6 mm and 110 mm length, be used as a cover plate for the creation of pores on the paver block. The plate has a dimension of 290 mm length and 160 mm breadth. Figure 7 and 8 represents the MS spikes arrangements in which they are welded on the other side of the metal plate. Figures 9 show the cross-sections of the plate.



Fig .7Mild steel cover plate

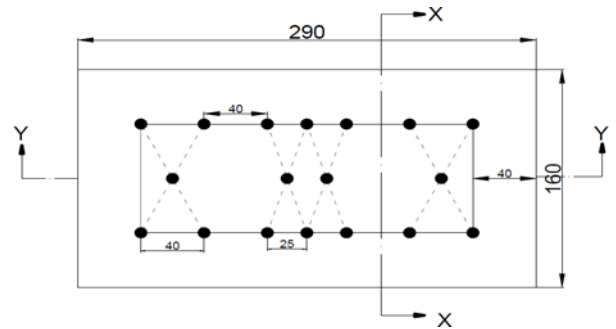


Fig .8 Top View (Plan) of Cover Plate

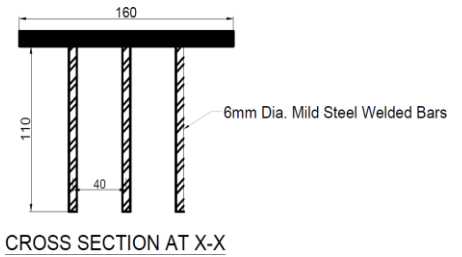


Fig .9 Cross Section at X-X of Cover Plate

10) *Rubber Paver Block Mold:* Rubber paver block mold (Dented Type – A as per IRC SP 63 – 2016[17]) of clear dimensions 250 mm length, 120 mm breadth, and 100 mm depth with 10 mm thickness is used for casting the paver blocks. Irregular roughness can be given on the bottom surface of the mold to ensure adequate friction. Figure10 represents the top view of the paver block mold with a cover plate. Figure 11 represents the top view of the paver block with an MS cover plate on it.

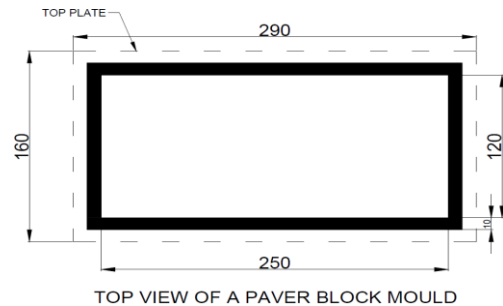


Fig. 10 Paver Block Mold with Cover Plate

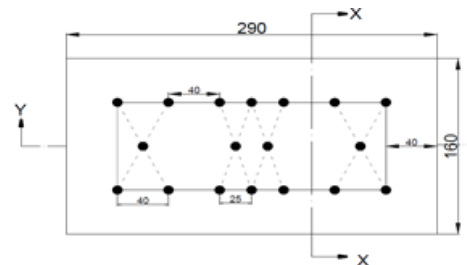


Fig .11 Paver Block Mold with Top Plate showing Mild Steel Spikes at the Bottom



Fig .12 Dented Type-A Interlocking Paver Block
Mold with Straw.

D. Concrete Mix Design:

1) *Mix Design:* Fly ash used in the project is brought from UPCL, Padubidri. GGBS is brought from Quality Polytech, Baikampady, Mangalore. Coarse and fine aggregate is brought from a quarry in Karkala. sodium silicate solution and Sodium hydroxide (NaOH) flakes are brought from a chemical shop in Udupi. M-45 mix design was done by using the conventional method (IS-10262: 2019)[18] and the same was improved according to the existing literature to develop the mix design for sustainable pervious concrete. The mix design per cubic meter, obtained are shown in table 3.

TABLE III
TABLE 3. MIX DESIGN PROPORTIONS (FOR 1 M³)

Material	Quantity (kg)
1. Ground Granulated Blast Furnace Slag (GGBS)	330
2. Fly Ash	110
3. Alkaline Solution:	
4. Sodium Silicate Solution	83.84
5. Sodium Hydroxide Flakes	12.484
6. Water	43.983
Total	=140.307
7. Additional Water	132
8. Coarse Aggregate	1052.2
9. Fine Aggregate	649.82

2) *Mix Design Procedure:* The following step-by-step procedure is used while mixing the ingredients for paver blocks.

1. A mix design was prepared with reference to field conditions and literatures.

2. Coarse Aggregate (size 10mm), Fine aggregate (150 microns retained), GGBS, Fly ash were first dry mixed using hands, manually.

3. Alkaline solution and water is later added and mixed manually for 3min with proper observations to obtain a homogenous mix.

4. Then the concrete mix is quickly filled into the 100mm thick molds.

5. The concrete was infilled in 3 layers and vibrated over a table vibrator.

6. Then the steel cover plate is inserted into the concrete mix so that pores are created on the paver block.

7. After a few minutes, the cover plate is taken off from the paver block and the block is allowed for air curing.

8. The procedure is repeated for casting another set of blocks.



Fig .15 Paver Block kept for Air Curing.

3) *Mixing, Casting, And Curing Procedure:* The materials are mixed thoroughly till a homogenous mix is obtained. The mix proportion is obtained from the extensive literature survey for the sustainable pervious concrete. After the concrete is filled into the mold and once the compaction, insertion, and removal of the cover plate are over, the block is kept for air curing. The investigation on the Compressive strength, on specimens of 100 mm thick is carried out for the desired mix proportion.

4) *Compressive Strength Test:* one of the most important property of concrete is *Compressive strength*. The compressive strength of the concrete is measured in N/mm². The compressive strength depends on various factors like material/water ratio, degree of compaction, type, and quality of binding material, type, and texture of aggregate, temperature, curing. The compressive strength test is carried out as per IS 516-1959 [19]. The specimens after air curing for 28 days are subjected to a compressive strength test. The specimens are kept in the compression testing machine in such a way that the load was imposed on the opposite side of the cubes. Then the load was gradually applied without shock. The maximum load applied is noted and the compressive strength of the concrete is calculated by the following formula:

$$\text{Compressive strength, } f_c = P/A \text{ N/mm}^2 \tag{1}$$

Where P = Applied Load in N

A = Surface area of cube



Fig .16 Compressive Strength Test of 100X100X100 mm Specimen

5) *Compression Test on Pervious Paver Block:* The test is carried out concerning IS 15658 - 2021[20] and the following steps were followed:

1. Tests are conducted after curing for 76 days
2. Cubes are tested in a compression testing machine with a maximum capacity of 200 tones.
3. Load is imposed without shock, uniformly and incessantly at a rate of 14N/mm² until the cube fails under the load.
4. Ultimate load applied on the specimen is noted down.
5. The formula used for calculating the compressive strength is

Compressive strength (N/mm²) = Ultimate Load/ Area sections.



Fig.17 Mode of Failure of Pervious Paver Blocks

6) *Results:* The compressive strength of paver blocks obtained for 76 days was 41.77 N/mm². The compression strength of the paver block (designed as per IRC 44-2017[21]) for 76 days was found to be 11.33 N/mm².

IV. CONCLUSIONS

The experimental study has been carried on alkali-activated pervious concrete paver block. From the results obtained, the following conclusions can be drawn:

- Sustainable Pervious Paver Block in which the pores are induced using cover plates has higher compressive strength than the pervious paver block designed as per IRC 44-2017[21].

- Pervious Paver Blocks can be used for low volume roads and also for effective rainwater management, drainage water management in urban areas.

ACKNOWLEDGMENT

This work is carried out at the Department of Civil Engineering NMAMIT-Nitte Authors would like to gratefully acknowledge the HOD and principal of the institute.

REFERENCES

- [1] M. Kamath, S. Prashant, and M. Kumar, "Micro-characterisation of alkali activated paste with fly ash-GGBS-metakaolin binder system with ambient setting characteristics," *Constr. Build. Mater.*, vol. 277, pp. 1–37, 2021, doi: 10.1016/j.conbuildmat.2021.122323.
- [2] B. Debnath and P. P. Sarkar, "Pervious concrete as an alternative pavement strategy: a state-of-the-art review," *Int. J. Pavement Eng.*, vol. 21, no. 12, pp. 1516–1531, 2020, doi: 10.1080/10298436.2018.1554217.
- [3] L. Monfardini and F. Minelli, "Experimental study of alkali activated concrete : Structural applications Experimental study of alkali activated concrete : Structural applications," in *International Conference on Applied Mineralogy & Advanced Materials*, 2015, pp. 1–6, doi: 10.14644/amam.2015.011.
- [4] A. K. Chandrappa and K. P. Biligiri, "Pervious concrete as a sustainable pavement material-Research findings and future prospects: A state-of-the-art review," *Constr. Build. Mater.*, vol. 111, pp. 262–274, 2016, doi: 10.1016/j.conbuildmat.2016.02.054.
- [5] R. Patil, "Pervious concrete: properties advantages & disadvantages.," *CONSTRUCTIONOR*. [Online]. Available: <https://constructionor.com/pervious-concrete/>.
- [6] A. K. Chandrappa and K. P. Biligiri, "Investigation on flexural strength and stiffness of pervious concrete for pavement applications," *Adv. Civ. Eng. Mater.*, vol. 7, no. 2, pp. 1–22, 2018, doi: 10.1520/ACEM20170015.
- [7] H. El Hassan and P. Kianmehr, "Pervious concrete pavement incorporating GGBS to alleviate pavement runoff and improve urban sustainability," *Road Mater. Pavement Des.*, vol. 19, no. 1, pp. 167–181, 2018, doi: 10.1080/14680629.2016.1251957.
- [8] S. Hesami, S. Ahmadi, and M. Nematzadeh, "Effects of rice husk ash and fiber on mechanical properties of pervious concrete pavement," *Constr. Build. Mater.*, vol. 53, pp. 680–691, 2014, doi: 10.1016/j.conbuildmat.2013.11.070.
- [9] S. Muthukumar, A. Jai Saravanan, A. Raman, M. Shanmuga Sundaram, and S. Sri Angamuthu, "Investigation on the mechanical properties of eco-friendly pervious concrete," *Mater. Today Proc.*, pp. 1–6, 2020, doi: 10.1016/j.matpr.2020.10.333.
- [10] N. Palankar, B. M. Mithun, and A. U. Ravishankar, "Alkali Activated Concrete with Steel Slag Aggregate for Concrete Pavements," *Int. J. Eng. Technol.*, vol. 7, no. 3.34, pp. 818–822, 2018, doi: 10.14419/ijet.v7i3.34.19568.
- [11] S. Marathe, I. R. Mithanthaya, and R. Y. Shenoy, "Durability and microstructure studies on Slag-Fly Ash-Glass powder based alkali activated pavement quality concrete mixes," *Constr. Build. Mater.*, vol. 287, pp. 1–18, 2021, doi: 10.1016/j.conbuildmat.2021.123047.
- [12] R. Zhong and K. Wille, "Material design and characterization of high performance pervious concrete," *Constr. Build. Mater.*, vol. 98, pp. 51–60, 2015, doi: 10.1016/j.conbuildmat.2015.08.027.
- [13] Y. Zhang, H. Li, A. Abdelhady, and J. Yang, "Comparative laboratory measurement of pervious concrete permeability using constant-head and falling-head permeameter methods," *Constr. Build. Mater.*, vol. 263, pp. 1–11, 2020, doi: 10.1016/j.conbuildmat.2020.120614.
- [14] S. Wang, G. Zhang, B. Wang, and M. Wu, "Mechanical strengths and durability properties of pervious concretes with blended steel slag and natural aggregate," *J. Clean. Prod.*, vol. 271, pp. 1–34, 2020, doi: 10.1016/j.jclepro.2020.122590.
- [15] A. K. Chandrappa and K. P. Biligiri, "Effect of pore structure on

Development Of Alkali Activated Pervious Concrete Paver Blocks

- fatigue of pervious concrete,” *Road Mater. Pavement Des.*, vol. 20, no. 7, pp. 1525–1547, 2019, doi: 10.1080/14680629.2018.1464500.
- [16] “IS:2386 Method of Test for aggregate for concrete. Part III- Specific gravity, density, voids, absorption and bulking.” Bureau of Indian standards, New Delhi, pp. 1–22, 1963.
- [17] “IRC:SP:63-2016 Guidelines for the use of interlocking concrete block pavement.” Indian Roads Congress, New Delhi, pp. 1–48, 2016.
- [18] “IS 10262:2019 Concrete Mix Proportioning- Guidelines.” Bureau of Indian standards, New Delhi, pp. 1–44, 2019.
- [19] “IS:516 Method of Tests for Strength of Concrete.” Bureau of Indian standards, New Delhi, p. New Delhi, India, 2004.
- [20] “IS 15658:2021 Indian Standard Precast Concrete Block for Paving- Specification,” *Bureau of Indian Standards*. Bureau of Indian standards, New Delhi, pp. 1–27, 2021.
- [21] “IRC 44:2017 Cement Concrete Mix Design.” Indian Roads Congress, New Delhi, pp. 1–64, 2017.

A Review on Extraction, Purification and Structural Characterization of Plant Polysaccharides

Pannaga K N¹, Darshini S M² and Vidya S M^{3,*}

^{1,2} Research Scholars, Department of Biotechnology Engineering, NMAMIT, Karkala, Udupi, Karnataka – 574-110, Affiliated to VTU, Belgaum.

³ Professor, Department of Biotechnology Engineering, NMAMIT, Karkala, Udupi, Karnataka – 574-110, Affiliated to VTU, Belgaum.

¹kulkarni.pannaga@gmail.com

²darshinism12@gmail.com

^{3,*} drvidyasm@nitte.edu.in

Abstract-Polysaccharides are versatile in nature having numerous medicinal values and being non-toxic with no side effects. This property has made its scope to attract the attention of various pharmaceutical industries and biomedical field since few decades. Polysaccharides are shown to be derived from various natural and synthesized resources and have proven to be a boon to the mankind. Studies on polysaccharides has demonstrated the biological effects such as immunomodulatory, anti-mutant, anti-diabetic, antibiotic, anticoagulant, anti-inflammatory, radioprotective effect, anti-viral and hypolipidemic activities of it. It has also proved to be one of the efficient antioxidant showing free radicals elimination, lipid peroxidation and have anti-aging effects. The polysaccharides have proved its potentiality in drug delivery, tissue engineering and regenerative engineering as well. In order to isolate, purify and characterize the polysaccharides from various natural and synthetic sources there are several physical, chemical and biological methods followed. Bioactive polysaccharides have acquired significant attention from scientists as they can be explored as functional biomolecules in the development of innovative and value-added products in the fields of pharmaceuticals, food, cosmetics and biomedical industry. Their therapeutic application is mainly due to their bio-degradable, non-toxic and bio-compatible nature. Extraction and isolation of naturally occurring bioactive polysaccharides possessing high purity with maximum extraction yield, by not disturbing its native structure are of great future concern and remains a field for further exploration. Therefore, this review paper tries to bring together all information about extraction, purification and structural characterization of polysaccharide.

Keywords- Plant polysaccharides, extraction, purification, molecular weight, structural characterization.

I. INTRODUCTION

Polysaccharides that are derived from plant sources constitute large family of biopolymers and are widely distributed in nature. Many of these polysaccharides have a long history as part of herbal ingredients that have been widely accepted in Asian countries. Polysaccharides can be found in nature in almost all parts of plants including tissues of seeds, stems, roots and leaves in plants. They range in structure from linear to highly branched which includes storage polysaccharides such as starch; structural polysaccharides such as cellulose, pectin. The major sources of galactomannan polysaccharide present in seeds of locust bean (*Ceratonia siliqua*), guar (*Cyamopsis tetragonoloba*), tara (*Caesalpinia spinosa Kuntza*), and fenugreek (*Trigonella foenum-graecum L.*). Polysaccharide glucomannan mainly present in the tuber or root of the elephant yam, also known as konjac (*Amorphophallus konjac*). They are polymeric carbohydrate macromolecules composed of long chains of monosaccharide units which are joined by glycosidic linkages. There are two types of polysaccharides such as homo-polysaccharides and hetero-polysaccharides. Homo-polysaccharides will be having only one type of monosaccharide unit repeating in the chain, whereas hetero-polysaccharide is composed of two or more types of monosaccharides as illustrated in Fig.1 below. Homo-polysaccharides can be branched or unbranched as long as they all have the same monosaccharide units. Among both, the monosaccharide can link in a linear fashion and they can branch out into complex formations. There are various studies conducted from last few decades with the aim of exploring their specific bioactivities towards human health. The majority of polysaccharides are mainly used alone or in combination with other compounds. Previous studies have also shown that medicinal plant polysaccharides are non-toxic and show no side effects.

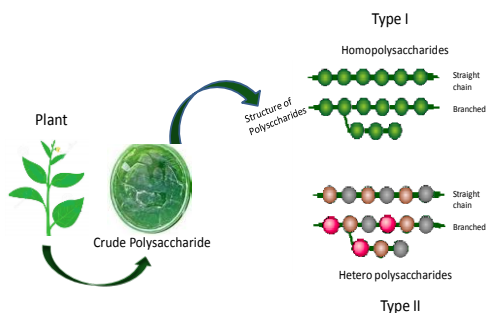


Fig. 1

Structure of homo and hetero polysaccharides

Based on these encouraging observations, most researches have been focusing on the isolation and identification of polysaccharides, as well as their bioactivities. A large number of bioactive polysaccharides with different structural features and biological effects from medicinal plants have been purified and characterized so far. The biological activities of polysaccharides are correlated with their structural characterization. The type of monomer, linkage type and position, number and position of branches occurring within the polymer chain strongly influence the three-dimensional arrangement; and are the factors which determine polysaccharide behavior in addition to the molecular size. Physical properties such as solubility, viscosity, gelation may also affect the biological activity as they influences its bioavailability. Some studies have suggested that polysaccharides have significantly different molecular weights; however fractions with similar monosaccharide compositions can display the same biological activity (Luo *et al.*, 2010). Therefore, elucidation of molecular structures of polysaccharides occurring in medicinal plants is very important for predicting their biological behavior.

In an earlier studies, a neutral polysaccharide was isolated from the water extract of leaves of *Litsea gardneri* and found to be composed mainly of xylose (70%) and small or approximately equimolar amounts of arabinose, mannose, galactose and glucose. Methylation 3[C] NMR spectroscopy of the native and degraded polysaccharides indicated the presence of a 1→4 linked β-Deoxylopyranosyl backbone. It is possible that some arabinofuranosyl residues were incorporated in the backbone of the polymer. Side chains were attached to O-2 of some of the xylopyranosyl residues in the polymer chain. The available evidence suggests that the side chains may be either single units of terminal arabinofuranosyl/ xylopyranosyl residues or multiple unit side chains containing both arabinosyl and xylosyl residues (Swarna and Savitri, 1995). Isolation of polysaccharides from such polysaccharide complex cellular plant matrices without disturbing its structure by keeping their bioactivity intact is at most important. During the last decade, various innovative green extraction techniques such as microwave-assisted, ultra-sonication, super critical fluid extraction and hot water extraction are in practice for isolation of bioactive polysaccharides.

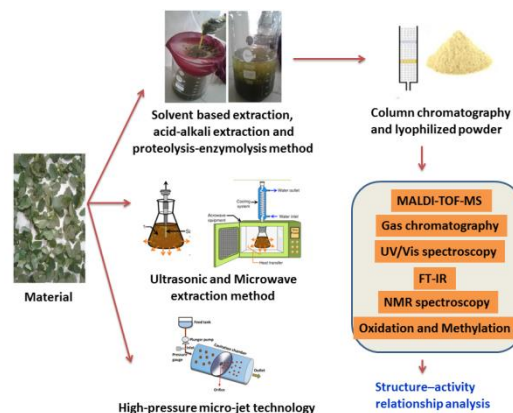


Fig. 2 Extraction and purification techniques involved during isolation of polysaccharides

These techniques have acquired great attention for scientists and researchers because of their increased extraction rates, cost-effective nature, enviro-friendly characteristics and structure preservative potentials. The type of method adopted defines the physicochemical properties and antioxidant potential of isolated polysaccharides. The hot water extraction method used in combination with various latest techniques like enzymatic pre-treatment, microwave and ultrasound-assisted are useful in increasing the yield and extraction productivity of polysaccharides. Likewise, enzymatic pre-treatment of raw material prior to the extraction resulted in reduced extraction time, minimized the use of extraction solvents, preserved the bioactivities of the polysaccharides and was energy efficient as compared to non-enzymatic pre-treated techniques. Recently various ionic liquids have been formulated which aids in extraction of polysaccharides in a shorter time and at lower temperatures. Fig. 2 explains various extraction and purification techniques which are available for isolation of polysaccharides from plant material.

II. LITERATURE SURVEY

A. Extraction of polysaccharides

Effective separation and purification of polysaccharides are the key steps outlining the consensus. The quality and function of polysaccharides can vary significantly due to differences in their origin, region of production and cultivation conditions. They are macromolecules with large molecular weight and complex structure; hence pose great challenge for the analytical technologies. The macromolecular configurations of plant cellular polysaccharides, particularly hetero polysaccharides like hemicelluloses are very complex owing to the occurrence of various monosaccharides acting as isobaric stereoisomers (Maki *et al.*, 2011). Additionally, polysaccharides present in plants are chemically or physically bound with various other biomolecules like lignin, proteins, lipids, polynucleotides and few minerals.

Polysaccharides are polar molecules that are often soluble in water but insoluble in organic solvents. Therefore, water is currently the most common extraction solvent and the base solvent of other extraction methods, including acid-alkali extraction and enzymolysis method. The main principle of

polysaccharide extraction is to break the cell wall from the outside to the inside under mild conditions, thus avoiding denaturation of polysaccharides. The yield obtained by water extraction method can be drastically increased by increasing the water temperature. Extraction yield was directly proportional to extraction time. The influence of temperature on the extraction yield might be due to water to plant material ratio, extraction time, more solvent to liquid ratio. When the solvent to water to plant material ratio reached at least 2:1 or above the extraction yield was the highest, and further increasing the ratio did not show increase in yield. Whereas, extraction yield of microwave assisted method was higher than water extraction method with conventional heating (Michael *et al.*, 2016). Maximum yield of polysaccharides were obtained from *Tamarindus indica* Linn. seeds with increased temperature and time.

Once the polysaccharides are extracted deproteinization should be done by the Sevag method. The protein clearance rate with the Sevag method will be similar to that with the trichloroacetic acid method, but had only half of the polysaccharide retention rate of the trichloroacetic acid method. There will be significant loss in the recovery of polysaccharides, which may be due to damage to the polysaccharides by the Sevag reagent as well as the co-removing effects of the glucoprotein during the harsh chemical treatment procedure (Peng *et al.*, 2016). Hence, trichloroacetic acid method remains most effective approach to eliminate the protein giving the highest protein clearance rate and polysaccharide retention rate among the tested methods. Whereas hydrochloric acid method will cause partial hydrolysis of polysaccharides which results in reduced polysaccharide retention rate (Liu *et al.*, 2010).

Mechanochemical extraction method was used to successfully extract polysaccharides using water as solvent; the process remains simple, fast upto 40sec and gives high yield. The molecular weight of the intact saccharides from calibration curve and light scattering measurement were determined and compared after separation with size exclusion chromatography. In an another study, air dried powder of plant sample (40 g) was extracted with 95% ethanol (1 L) at 90°C in a water bath for 5 h under stirring to remove pigments, polyphenols and monosaccharides. As the liquid cooled, it was centrifuged at 5000 rpm for 15 min at 4°C. This was repeated thrice and the supernatants were combined and concentrated in a rotary evaporator under reduced pressure and then filtered. The concentrated solution was deproteinated by the Sevag method, trichloroacetic acid method, and hydrochloric acid method, with each method repeated six times. The solution was further decolorized by the macroporous resin separation method. Hyperfiltration was applied to desalinate with a molecular weight membrane of 3 KDa and at a flow rate of 5.0 mL/min for 8 h. After that, the filtrate was precipitated by adding 99.5% ethanol four times the volume of the aqueous extract at room temperature for 8 h, and then centrifugation at 4000 rpm for 10 min at 4°C. Finally, this was dissolved in distilled water and then lyophilized in a vacuum freeze dryer to obtain the crude

polysaccharide. A sample of the polysaccharide (200 mg) was redissolved in distilled water, and then purified with the DEAE-cellulose A52 column (2.6 cm × 60 cm), which was equilibrated with distilled water. The polysaccharide was fractionated by stepwise elution with distilled water, followed by a gradient elution with aqueous NaCl (0–0.5 M) at a flow rate of 1.0 mL/min. Fractions (5 mL) were collected and the absorbance at 490 nm was measured using the phenol-sulfuric acid method (Gabriela *et al.*, 2003). The eluted solution was separated into two fractions of polysaccharides, which were further purified on the Sephadex G-100 gel filtration column (2.6 cm × 60 cm), and eluted with deionized water at a flow rate of 9 mL/h. The eluate was concentrated, dialyzed against water and lyophilized to obtain white powder of pure polysaccharides.

In ultrasonic extraction method the ultrasonic wave cavitation is used to break cell walls and accelerate the dissolution of organics in cells, thus improving the yield of polysaccharides. Zhu *et al.* used ultrasound waves to extract polysaccharides from *Polygonum multiflorum*, achieving a maximum extraction rate of 5.49%. After separation and purification, both neutral and acidic components showed high anti-tumor activity. Recent research suggested that the ultrasonic extraction method could significantly improve the rate of polysaccharide dissolution, whereas prolonged exposure to ultrasound may change the advanced structure of polysaccharides and affect the biological activity.

In case of microwave extraction, when the cell absorbs microwave energy the intracellular pressure will increase leading to cell rupture and causing the active components to flow into the solvent (Silva *et al.*, 2018). The microwave assisted extraction method can improve the yield of polysaccharides significantly. For instance, the yield of polysaccharides from *Cyphomandra betacea* was determined to be high under the optimal conditions (Kumar *et al.*, 2016). However, a rapid temperature spike may change the molecular mass distribution and the structures of the thermally unstable polysaccharides. Extraction using CO₂ in the supercritical state can be done to selectively extract components of a mixture due to differences in their polarity, boiling point and molecular weight. It is based on the relationship between the solubility in the supercritical fluid and the density. In this system, the use of appropriate entrainers and modulators (e.g., methanol and ethanol) can also improve the rate of extraction of polysaccharides. Supercritical CO₂ fluid has good solvency and high efficiency in analytical procedures.

Subcritical water extraction has been successfully applied for extraction of the active components of natural products. Yang *et al.* compared the extraction rate of *Lycium barbarum* fruit polysaccharides by using hot water extraction, ultrasonic extraction, subcritical water extraction and ultrasound combined with subcritical water extraction, respectively. The results showed that the extraction rate achieved with ultrasound combined with subcritical water extraction was high. Although

the application of subcritical water extraction to natural polysaccharides is still in the stage of basic research and has not reached the level of industrial production, this method can be used to extract polysaccharides with better quality and maintain higher activity. Another emerging technology is dynamic high-pressure micro-jet technology which combines shear, high-frequency vibration, cavitation and instantaneous pressure drop with a maximum pressure of 200 MPa. Although this method has the obvious advantages of a short extraction time and high extraction rate it is possible to break the polysaccharide chain and change its original characteristics. Due to the opaque heating from infrared radiation, this method offers high permeability, which is conducive for effective dissolution of the cell components. Infrared radiation is increasingly applied to the auxiliary extraction of active components from natural products. This method has the advantages of a short extraction time, low temperature operation, free irradiation and low cost. Considering the diversity and complexity of the extracted polysaccharides, such as snow chrysanthemum polysaccharides, increasing attention has been focused on the cooperative utilization of multiple technologies, where each method is exploited to maximize the effectiveness (Guo *et al.*, 2019). Therefore, appropriate extraction methods should be employed for retaining the inherent properties of polysaccharide molecules and preventing chain fracture and changes in the spatial conformation.

B. Purification of polysaccharides

Polysaccharides after being removed from cell are not a single molecule but a mixture with different degrees of polymerization. Therefore, deep purification is the basis for studying the relationship between the structure and the biological activity. Based on the separation mechanism the purification techniques can be divided into three categories i.e. physical, chromatographic and chemical precipitation. It is difficult to rely on single purification method and the combination of several separation methods and several devices has been employed to improve the purification results. In addition, this purification of polysaccharides from the crude extract is really of great importance as the linkage among structure and safety of products formed for food, pharmaceutical and biomedical application depends on this. Purification could be achieved by using various techniques like gel filtration, ion exchange and affinity chromatography, ethanolic precipitation and fractional precipitation individually or in combination (Thakur *et al.*, 2012).

As discussed above the conventional methods for protein removal are Sevag method and the trichloroacetic acid method based on the principle that the reagent denatures and precipitates proteins instead of polysaccharides. However, the Sevag method is complicated and time-consuming. Apart from the direct addition of a common protease for protein removal, microorganisms like *Saccharomyces cerevisiae* can be used to remove proteins. In order to compensate the deficiency of a single method, the Sevag-enzyme combination could effectively reduce the loss of polysaccharides. The phenolic compounds present during the extraction of natural

polysaccharides produce pigments. The pigments present affect the chromatographic analysis and impede accurate identification of the polysaccharides due to oxidation. In particular, the crude polysaccharides from animals are darker than those from plants. Decolorization processes usually include resin method, activated carbon method and hydrogen peroxide oxidation method. Specifically, the ion exchange resin or the adsorption resin acts advantageous having high decolorization rate and stable characteristic group structures.

Column chromatography is an efficient purification method for the separation and the purification of natural components. Based on the physicochemical properties of the target substance, the most suitable stationary phase and mobile phase are selected for achieving high yield of the target substance. Column chromatography can be divided into cellulose column chromatography, ion exchange column chromatography, gel column chromatography and affinity column chromatography. Diethylaminoethyl (DEAE) cellulose anion exchange column chromatography and gel column chromatography have been used in tandem to purify polysaccharides (Xu *et al.*, 2012). Anion exchange column chromatography is generally used as the primary stage for the purification of crude polysaccharides and is based on the principles of adsorption and partition chromatography (Xie *et al.*, 2013; Shi *et al.*, 2013). Similarly, gel column chromatography is based on the molecular sieve action of the gel which has porous network structure in three dimensions. It depends on the speed of motion of the polysaccharides with different molecular sizes and shapes in the chromatography column.

C. Determination of homogeneity and relative molecular weights

The homogeneity and molecular weights of polysaccharides are determined by gel permeation chromatography and multi-angle laser light scattering (GPC/MALLS). The samples are diluted with ultrapure water and filtered through a 0.45 µm membrane on the GPC/MALLS instrument, and eluted with 0.1 M NaNO₃ and 0.02% sodium azide at a flow rate of 0.5 mL/min. A refractive index detector is used for detection at 40°C. The molecular weights of polysaccharides are estimated by reference to a calibration curve constructed using the dextrans of known molecular weights. Usually gas chromatography (GC) is used for identification and quantification of the monosaccharide units in polysaccharide. First, Polysaccharide is hydrolyzed with 2 M trifluoroacetic acid (TFA) (2 mL) at 120°C for 2h. Excess acid is completely removed by distilled water and then hydrolyzed products are mixed with 2 mL of pyridine, immediately followed by 0.4 mL of trimethylchlorosilane, and 0.8 mL of hexamethyldisilazane. The mixture is shaken in a 50°C water bath for 15 min to dissolve the solute. Then, 1.5 mL of deionized water was added. After the solution had separated out, the supernatant was isolated by centrifugation at 3000 rpm for 10 min. Standards such as arabinose, rhamnose, ribose, xylose, mannose, galactose and glucose are also prepared in the same way and subjected to GC analysis separately. The impurity content of the polysaccharide is determined in quartz colorimetric utensil

using UV/Vis spectroscopy at an optical path length of 1 cm and a scan interval of 1 nm. The spectrum of polysaccharide (1 mg/mL) are recorded in the region 200–400 nm at 25°C. Organic functional groups and the primary structure of polysaccharide are identified according to the spectrum of FT-IR. For FT-IR, polysaccharide (3 mg) are dried at 35–45°C under vacuum, then ground to a powder with spectroscopic grade KBr. The powder is pressed into a 1 mm pellet and spectra are recorded from 400 to 4000 cm⁻¹ with a resolution of 8 cm⁻¹ resolution and 32 scans at 25 °C. The spectrum performed a smoothing and a correction of the baseline by using Origin 8.6 software.

The locations of glycosidic linkages in polysaccharides can be preliminarily determined by periodate oxidation in which periodate will be consumed and formic acid will be produced (Ruijun *et al.*, 2015). Polysaccharides (10 mg of each) were oxidized with 0.15 M NaIO₄ (40 mL) and kept in the dark and absorption was monitored at 223 nm every 4 h. Complete oxidation, identified by a stable absorbance, reaches in 96 h, and excess NaIO₄ is removed at this time by adding ethylene glycol. Consumption of NaIO₄ is measured by a spectrophotometric method, and formic acid production is determined by titration with 0.005 M NaOH. Methylation analysis of polysaccharides can be done according to the method of Needs and Selvendran (Needs and Selvendran, 1993). The methylated products are extracted into chloroform and examined by FT-IR. The absence of a hydroxyl absorption peak indicates the completion of methylation. The methylated products are hydrolyzed with formic acid and 2 M TFA for about 2 h, and excess acid is removed by co-distillation with distilled water or methanol. Each hydrolysate was combined with 2 mL of acetic anhydride and 2 mL of pyridine and heated at 100°C for 1 h. After acetylation with acetic anhydride, product is analyzed by gas chromatography-mass spectrometry (GC-MS) on an GC 7890 N gas chromatograph coupled with an mass-selective detector. The GC-MS conditions will be as follows: The GC capillary column was DB-1701 (0.25 mm × 30 m, 0.25 mm) and the mass scan range is 30–450 m/z (electron ionization 70 eV). The injector and detector are operated at a temperature of 220° C and 280° C, respectively. Temperature program is programmed as follows: initial temperature of 150° C was held for 3 min and then increased to 260° C by 15° C/min and held for 5 min. Helium was used as the carrier gas with a constant flow rate of 1 mL/min. MALDI-TOF-MS is often used to analyze biological macromolecules. The collision-induced cleavage, electron transfer cleavage, electron capture cleavage, post-source decay and other post-source cleavage techniques are not only used for determination of the molecular weight of polysaccharides but also for identification of the structural fragments (Guo *et al.*, 2012). In the measurement process, the matrix and the sample concentration are selected according to the structure of the polysaccharide to achieve desired result.

D. Structural characterization of polysaccharides

The uniqueness in physiochemical properties, structure diversities and biological effects of polysaccharides can be used successfully in great numbers of medical applications. Many bioactive polysaccharides have presented promising potential as antitumor, immune stimulating and as anticancer agents. This area of research has attracted a lot of interest also due to the fact that these polysaccharides are produced by medicinal plants makes them very good candidates for good medicines without any serious safety concerns as they are often eaten in the diet. The structural features and bioactivities have been widely explored from medicinal plants, and the structural diversity of polysaccharides depends largely on their botanical or biological sources. Structural analysis of polysaccharides behaves promising and crucial for elucidating structure–activity relationships. Polysaccharides, derived from multiple natural resources such as plants, animals, bacteria, fungi, algae, arthropods, etc., are not only an important component of energy and structural components but also serve a variety of biological functions. Many of these functions include recognition of signals, intercellular connection, regulation of immune system, coagulation of blood and inhibition of pathogens. Nevertheless, polysaccharides are still a mystery because its structure–activity relationship is unclear; and polysaccharide detection and quantification has not been standardized. Although the synthesis of polysaccharides has undergone significant developments, limited by their structure complexity, it is still challenging and time consuming to pursue the synthetic route due to the lack of commercial automated synthesizers and difficulties in controlling the stereochemistry of the glycosidic linkages (Xiao and Grinstaff, 2017). Effective separation and purification is the preconditions for structural identification and study of the structure–activity relationship as well (Shi, 2016). For structural analysis, in terms of glycosidic linkage are analysed using nuclear magnetic resonance (NMR) systems such as proton NMR (1 H), carbon NMR (13C), 1 H - 1 H correlated spectroscopy (COSY), 1 H - 13C heteronuclear single quantum coherence spectroscopy (HSQC), 1 H - 1 H total correlated spectroscopy (TOCSY) and 1 H - 13C heteronuclear multiple bond correlation spectroscopy (HMBC).

III. CONCLUSION

Natural polysaccharides are prospectively the most precious wealth that nature has given us. The main focus of the review is on extraction, purification and characterization methods of polysaccharides from the plant source. As this class of biopolymers forms ideal candidates for therapeutic applications, there is no doubt that bioactive polysaccharides from the medicinal plants are going to take major place in future for biomedical applications. With the development of technology, interdisciplinary integration will provide many ideas and methods for polysaccharide identification and structure–activity relationship at the molecular level.

REFERENCES

- [1] Gabriela, C.; Norma, S.; Bessio, M.I.; Fernando, F.; Hugo, M. Quantitative determination of

- pneumococcal capsular polysaccharide serotype 14 using a modification of phenol-sulfuric acid method. *J. Microbiol. Methods* 2003, 52, 69–73.
- [2] Guo, Q., and Cui, S.W. (2014). Polysaccharides from *Dendrobium officinale*, *Cordyceps sinensis* and *Ganoderma*: Structures and bioactivities. In Williams PA, and Phillips GO (eds), *Gums and Stabilisers for the Food Industry 17- The Changing Face of Food Manufacture: The Role of Hydrocolloids*. Royal Society of Chemistry, Cambridge, UK, pgs. 303–318.
- [3] Kumar, C.S.; Sivakumar, M.; Ruckmani, K. Microwave-assisted extraction of polysaccharides from *Cyphomandra betacea* and its biological activities. *Int. J. Biol. Macromol.* 2016, 92, 682–693.
- [4] Liu, J.; Luo, J.; Sun, Y.; Ye, H.; Lu, Z.; Zeng, X. A simple method for the simultaneous decoloration and deproteinization of crude levan extract from *Paenibacillus polymyxa* EJS-3 by macroporous resin. *Bioresour. Technol.* 2010, 101, 6077–6083.
- [5] Luo, A.X.; He, X.J.; Zhou, S.D.; Fan, Y.J.; Luo, A.S.; Chun, Z. Purification, composition analysis and antioxidant activity of the polysaccharides from *Dendrobium nobile* Lindl.
- [6] Maki Arvela, P.I.; Salmi, T.; Holmbom, B.; Willfor, S.; Murzin, D.Y. Synthesis of sugars by hydrolysis of hemicelluloses—a review. *Chem. Rev.* 2011, 111, 5638–5666.
- [7] Michael Antony, Samy Amutha, Gnana Arasi¹, Manchineela Gopal Rao², Janardanan Bagyalakshmi³, The Comparison and Analysis of Two Extraction Methods for Polysaccharides in *Psidium guajava* L. Fruits, *Indian Journal of Pharmaceutical Education and Research*, 2016.
- [8] Needs P.W.; Selvendran, R.R. An improved methylation procedure for the analysis of complex polysaccharides including resistant starch and a critique of the factors which lead to undermethylation. *Phytochem. Anal. Needs*, 1993, 4, 210–216.
- [9] Peng, Y.; Han, B.; Liu, W.; Zhou, R. Deproteinization and structural characterization of bioactive exopolysaccharides from *Ganoderma sinense* mycelium. *Sep. Sci. Technol.* 2016, 51, 359–369.
- [10] Ruijun, W.; Shi, W.; Yijun, X.; Mengwuliji, T.; Lijuan, Z.; Yumin, W. Antitumor effects and immune regulation activities of a purified polysaccharide extracted from *Juglan regia*. *Int. J. Biol. Macromol.* 2015, 72, 771–775.
- [11] Shi, L. Bioactivities, isolation and purification methods of polysaccharides from natural products: A review. *Int. J. Biol. Macromol.* 2016, 92, 37–48.
- [12] Swarna Wimalasiri. K M & N. Savitri Kumar, A water-soluble polysaccharide from the leaves of *Litsea gardneri* (Lauraceae), Elsevier, (1995) 19-23.
- [13] Xiao, R.; Grinstaff, M.W. Chemical synthesis of polysaccharides and polysaccharide mimetics. *Prog. Polym. Sci.* 2017, 74, 78–116.
- [14] Zhu, Z.Y.; Liu, X.C.; Fang, X.N.; Sun, H.Q.; Yang, X.Y.; Zhang, Y.M. Structural and anti-tumor activity of polysaccharide produced by *Hirsutella sinensis*. *Int. J. Biol. Macromol.* 2016, 82, 959–966.
- [15] Zhu, W.L.; Xue, X.P.; Zhang, Z.J. Ultrasonic-assisted extraction, structure and antitumor activity of polysaccharide from *Polygonum multiflorum*. *Int. J. Biol. Macromol.* 2016, 91, 132–142.

Nasal Carriage of *Staphylococcus Aureus* among Orphanage Children in and around Mangalore

Dr. Radhakrishna M¹, Melreena Serra*², Udayalaxmi J¹

¹Manipal Academy of Higher Education, Manipal, Karnataka, India-576104¹

nidhi8996shree@gmail.com

²Department of Microbiology, Kasturba Medical College, Mangalore-575 001, India

*E-mail: melreena.serra@manipal.edu

Abstract— Introduction: Carriage of *S. aureus* in the nose plays a vital role in the epidemiology and pathogenesis of *S. aureus* infection. **Aim:** To determine the nasal carriage rate of *S. aureus* among orphanage children in Mangaluru, and its antibiotic sensitivity pattern. **Materials and methods:** Nasal swabs were collected from 234 orphanage children and inoculated into standard culture media. Isolates were identified by standard bacteriological methods. Antibiotic susceptibility testing for all the isolates of *S. aureus* was determined by modified Kirby Bauer disk diffusion method. Methicillin-resistant *Staphylococcus aureus* strains (MRSA) were detected by cefoxitin disc as per CLSI guidelines and confirmed by mec A gene detection by polymerase chain reaction (PCR). Minimum inhibitory concentration (MIC) for vancomycin and mupirocin was determined by E-test. **Results:** Out of the 234 nasal swabs collected, 90 (38.46%) were positive for *S. aureus*. The overall MRSA carriage rate was (15/234) 6.41%. The MIC of vancomycin for 15 MRSA isolates was found to be $\leq 1\mu\text{g/ml}$. Vancomycin MIC creep was not observed. MIC of mupirocin for 14 MRSA isolates were $< 4\mu\text{g/ml}$ and one was $\geq 512\mu\text{g/ml}$. Mec A gene was detected in all MRSA isolates. *S. aureus* isolates were 100% sensitive to Chloramphenicol, Linezolid and Teichoplanin. All isolates were 100% resistant to penicillin. MRSA isolates were in addition 100% sensitive to Clindamycin. **Conclusion:** Overall nasal carriage of *S. aureus* among orphanage children around Mangalore was 38.46% and MRSA 6.41%. There was no vancomycin-resistant *S. aureus* even though mupirocin resistance was observed in one isolate. Vancomycin MIC creep was not observed. orphanage children in Mangaluru, and its antibiotic sensitivity pattern.

Keywords: Orphanage, Child, Methicillin-resistant *Staphylococcus aureus*, Mupirocin, Polymerase chain reaction, Vancomycin.

I. INTRODUCTION

Staphylococcus aureus is the most common human pathogen, both in community and hospitals. It is also a common colonizer of the skin and nose. Anterior nares are the main reservoirs of *S. aureus* in children and adults. Carriage of *S. aureus* in the nose appears to play a key role in the epidemiology and pathogenesis of infection.^{1,2} The incidence of community-acquired and hospital-acquired *S. aureus* infection has been rising with increasing emergence of drug-resistant strains. Methicillin resistance in *Staphylococcus* is due to the presence of mec A gene.^{1,2} It mediates a reduction in the affinity of β -lactams to the penicillin binding protein (PBP) receptors, resulting in the development of methicillin

resistant *S. aureus* MRSA.^{1,2} Increasing rates of MRSA may result from unwise use of antibiotics in the treatment of *S. aureus* in hospitals and the inevitable transmission of MRSA strains to community.^{1,2} Vancomycin has been the drug of choice from decades for serious methicillin-resistant *S. aureus* infections until the emergence of MRSA strains with high vancomycin minimum inhibition concentration.³ Mupirocin is used in treating superficial skin infections and treating nasal carriage hence in controlling the spread of MRSA. Mupirocin is bactericidal, and it is active against most strains of *S. aureus*. But recent studies have shown the emergence of MRSA strains with both low and high mupirocin resistance.^{4,5} This study aimed at determining the nasal carriage rate of *S. aureus* with particular emphasis on methicillin-resistant *Staphylococcus aureus* among children from orphanage home in and around Mangaluru. We also study the vancomycin and mupirocin resistance exhibited by the isolates.

II. EXPERIMENTS

A community based cross sectional study was conducted at eight orphanages in urban Mangaluru. A total of 234 children were included in the study. Nasal swabs from both the anterior nares of consenting children were taken with a sterile swab stick moistened with sterile physiological saline. All children above five years were included in the study and all children below five years were excluded.

Processing of the samples was done immediately within 2 h of collection. The swabs were inoculated onto mannitol salt agar (MSA) plates and incubated at 37° C for 18-24 hours. The growth of the organism was identified as *S. aureus* by using standard tests, such as colony morphology, gram stain, catalase test, slide coagulase, and tube coagulase test.⁶ The isolated strains of *S. aureus* were screened for methicillin susceptibility by a modified Kirby-Bauer disk diffusion method using cefoxitin (30 μg) discs on Mueller-Hinton agar (MHA). An inoculum with a density equivalent to McFarland's 0.5 standards (1.5×10^8 CFU/ml) was used. Isolates which showed inhibition zone sizes of diameter ≤ 21 mm were considered as MRSA strains.⁷ MIC for vancomycin and mupirocin was determined by E-test.⁷ Antibiotic sensitivity to all *S. aureus* isolates against other antibiotics like penicillin (10 units), ciprofloxacin (5 μg), amoxicillin/clavulanic acid (20/10 μg), erythromycin (15 μg), clindamycin (2 μg), chloramphenicol (30 μg), co-trimoxazole

(25 µg), ceftriaxone (30 µg), gentamicin (10 µg), linezolid (30 µg), and teicoplanin (30 µg) was determined by modified Kirby Bauer disk diffusion method. All antibiotic susceptibility tests were controlled by using *S. aureus* ATCC 25923, MRSA ATCC 29213 and MSSA ATCC 33591 strains. Antibiotic discs used were procured from Hi Media Laboratories Pvt., Limited, India. Antibiotic sensitivity testing and interpretation of the result was done according to CLSI guidelines⁷

E-test for MIC determination:

E test was performed MRSA isolates only by standard method as per CLSI guidelines.⁷ For vancomycin, MICs ≤ 2 µg/ml was considered susceptible; MICs 4–8 µg/ml regarded as intermediate and ≥ 16 µg/ml as resistant. For mupirocin, MIC falling between 8 and 256 µg/ml was taken a low or intermediate resistance, those showing ≥ 512 µg/ml as highly resistant and those isolates showing MIC < 4 µg/ml were interpreted as sensitive as per CLSI guidelines.⁷

Detection of mecA gene by Polymerase Chain Reaction

The polymerase chain reaction was performed with 20 µl of the reaction mixture. The reaction mixture contained 10X PCR buffer, 10 µM forward primer, 10 µl reverse primer, 5U of Taq DNA polymerase, 2µl template DNA. Amplification was performed in a thermocycler with initial denaturation at 94°C for 2 minutes, followed by denaturation at 94°C for 1 minute, annealing at 60°C for 1 minute, extension at 72°C for 1 minute, final extension at 72°C for 5 minutes. Polymerase chain reaction products were analyzed in 1.5% agarose gel in the 1×TAE buffer. DNA amplicons were stained with ethidium bromide and visualized using a gel mapping system. Primers and the reagents required for the PCR were obtained from Sigma Chemical Company, USA. Primers used in the experiment are listed in the table 1.⁸

Statistical Analysis

Data analysis was done using statistical package for the social sciences (SPSS) version 17. Chi-square test was used to compare data.

III. RESULTS

Data A total of 234 orphanage children of above five years were included in the study. The study population happened to fall in the age group between 6-8 years. Out of which 120 (51.3%) were males, and 114 (48.7%) were females. Out of 234, 90 children were positive for nasal carriage of *S. aureus* giving a carriage rate of 38.46%. Fifteen out of 90 isolates of *S. aureus* were MRSA (16.66%) which was confirmed by PCR, gel picture showing the presence of mecA gene in all the 15 MRSA isolates was shown in the fig. 1. Six out of 120 (5%) males and 9 out of 114 (7.9%) females harbored MRSA ($p > 0.05$). Overall MRSA carriage rate was 6.41%. Nasal carriage of coagulase-negative Staphylococcus (CoNS) being predominant 103 (44.01%) followed by *S. aureus* (38.46%), diphtheroids 14 (5.98%) and *Candida sp.* 6 (2.56%). Eighteen (17.4%) out of 103 CoNS were resistant to methicillin. Antibiotic susceptibility results of *S. aureus* is shown in fig. 2. *S. aureus* isolates were 100% sensitive to chloramphenicol, linezolid, teichoplanin. and resistant to penicillin G. All MRSA isolates were 100% susceptible to chloramphenicol, linezolid, teicoplanin and clindamycin. Minimum inhibitory concentration to vancomycin in all the 15 MRSA isolates was

found to be < 2 µg/ml and in mupirocin 14 were < 4 µg/ml and one was ≥ 512 µg/ml by E-test (Fig 3). The anterior nares of humans are the primary ecological niche of *S. aureus*.¹ The carriage pattern of *S. aureus* is three types. Approximately 20% of the individuals almost always carry one kind of strain, and they are called persistent carriers. A large proportion of the population (60%) harbours *S. aureus* intermittently, and the strains change with varying frequencies. Such individuals are called intermittent carriers. Finally, a minority of people (20%) who rarely carry *S. aureus* are called non carriers. The reasons for these differences in the colonization patterns are unknown.¹

The present finding of carriage rate of *S. aureus* among orphanage children from Mangaluru was significantly low when compared to the 41% and 52.3% to similar studies in children from Ethiopia and Chandigarh, India respectively and higher when compared to 12.9% and 6.3% from the reviews at Makati City and Ujjain, India respectively.⁹⁻¹² The overall MRSA carriage rate among orphanage children in Mangaluru was found to be on the higher side when compared with the results obtained from the other studies involving general children populations conducted at Andhra Pradesh (3%), Chandigarh (3.89%), Ujjain, India (1%), Ethiopia (5.6%) Makati City (1.29%).⁹⁻¹³ Some recent Indian studies on nasal carriage of *S. aureus* in school children showed 16.9%, 46.67%, and MRSA 2.9% and 7.6%.^{14,15} Recent studies showed 2.1% MRSA nasal carriage in old people, 6.7% to 14.2% in health care workers.^{16,17}

Age and gender had no significant association with the nasal carriage in this study whereas previous studies showed substantial variations in *S. aureus* nasal carriage with age.^{14,18} Hospitalization, skin maceration, repeated furuncles, prior antibiotic treatment, nose picking habit, overcrowding are the common risk factors involved in colonisation.¹ A study of risk factor in these children may be taken up in future studies. Eighteen (17.47%) out of 103 CoNS were resistant to methicillin, indicating the emergence of MRCoNS. It is of some concern because such strains may cause infection in a susceptible individual with predisposing factors.¹⁹

In a study conducted in Egypt 200 *S. aureus* isolates were collected, 80 (40%) from clinical samples and 120 (60%) from nasal carriage samples. They detected 11 (13.8%) VRSA among clinical isolates and 1 (0.8%) VISA from nasal swab. VRSA isolates were most resistant to ciprofloxacin (90.9%) and erythromycin (81.8%). Five isolates were resistant to all tested antibiotics: ciprofloxacin, clindamycin, erythromycin, linezolid, oxacillin, penicillin and trimethoprim-sulfamethoxazole. MRSA was found to constitute 43.8 % of clinical isolates. The MRSA colonization rate among community individuals was 43.6%, 42.9% among healthcare workers and 51.4% among patients.²⁰ In a study from Uttar Pradesh, India on nasal carriage of *S. aureus* in children, all *S. aureus* and MRSA isolates were sensitive to vancomycin with MIC < 2 µg/ml, whereas 23 *S. aureus* were found resistant to oxacillin with MIC value > 4 µg/ml. Resistance to penicillin and cotrimoxazole was highest, whereas all were sensitive to linezolid. MRSA showed 100% susceptibility to linezolid, followed by gentamicin (91.4%) and tetracycline (87%).¹⁵

Another study from Uttar Pradesh on nasal carriage of *S.aureus* in health care workers, nearly 60% of MRSA were resistant to clindamycin and erythromycin and around 50% were resistant to tetracycline and co trimoxazole. MSSA isolates sensitive to penicillin were 23%, nearly 60% were sensitive to clindamycin, ciprofloxacin and levofloxacin and around 50% were sensitive to tetracycline and co trimoxazole. All isolates were susceptible to linezolid. Resistance to most of the antibiotics was significantly associated with MRSA strains ($P < 0.05$). Mupirocin resistance was seen in 4 (7%) of 28 MRSA isolates by E-test; 3 (75%) isolates were MuH, and 1 (25%) isolate was MuL. No mupirocin resistance was detected in MSSA. The MuH strains were isolated from the nasal swabs of nursing orderlies whereas the MuL strain was isolated from a nurse.²¹ In a recent study conducted in south India, mupirocin resistance was seen in 4.81% of clinical *S. aureus* isolates; all of which exhibited high-level resistance with MIC ≥ 1024 $\mu\text{g/ml}$.²² In the present study, all the *S.aureus* isolates were susceptible to chloramphenicol, linezolid, and teicoplanin and resistant to penicillin G. All MRSA isolates were susceptible to chloramphenicol, clindamycin, linezolid, teicoplanin. Which implies that the MRSA isolates were not multi-drug resistant. All 15 MRSA strains were sensitive to vancomycin, and one out of 14 MRSA strains was resistant to mupirocin. MRSA vancomycin MIC creep was not observed.

IV. CONCLUSIONS

The nasal carriage of *S.aureus* among orphanage children around Mangalore was 38.46%. The overall MRSA carriage rate was 6.41%. There was no vancomycin-resistant *S.aureus* and vancomycin MIC creep was not observed in MRSA isolates. MRSA isolates were 100% sensitive to chloramphenicol, clindamycin, linezolid, teicoplanin.

ACKNOWLEDGMENT

Financial support and sponsorship: Nil

Conflicts of interest: There are no conflicts of interest.

Ethical Consideration: The study was approved by the institutional Ethical Committee, Kasturba Medical College, Mangalore. IEC KMC MLR 01-17/25.

REFERENCES

- [1] Sakr A, Brégeon F, Mège J L, Rolain J M, Blin O. Staphylococcus aureus nasal colonization: An update on mechanisms, epidemiology, risk factors, and subsequent infections. *Front Microbiol.* 2018;9:2419. doi: 10.3389/fmicb.2018.02419.
- [2] Sahreena L, Kunyan Z. Methicillin-resistant Staphylococcus aureus: Molecular characterization, evolution, and epidemiology. *Clin Microbiol Rev.* 2018;31(4):1-103.
- [3] Holland T L, Fowler VG Jr. Vancomycin minimum inhibitory concentration and outcome in patients with *Staphylococcus aureus* bacteraemia: pearl or pellet. *J Infect Dis.* 2011; 204(3):329-31.
- [4] Nina K.A, Maria C G, Kimberly D M, Susan W, Paul J P, Christine T L. High prevalence of mupirocin resistance in *Staphylococcus aureus* isolates from a paediatric population. *Antimicrob Agents Chemother.* 2015;59(6):3350 -6.
- [5] Parul C, Amit Kumar S, Snehanushu S, Loveleena A. Prevalence of mupirocin resistant *Staphylococcus aureus* isolates among patients admitted to a tertiary care hospital. *N Am J Med Sci.* 2014;6(8):403-7.
- [6] Collee JG, Andrew G. Fraser, Barrie P. Marmion, Anthony Simmons: Mackie and McCartney practical medical microbiology 14th edition.2016;151-77.
- [7] CLSI. Performance Standards for Antimicrobial Susceptibility Testing (28th edition) Clinical and Laboratory Standards Institute; PA, USA: 2018. CLSI supplement M100: M100-S22.
- [8] Shahina S, Siddiqui S, Krishnan D. Nasal carriage of methicillin resistant staphylococci with inducible clindamycin resistance and Pvl gene. *Int J Sci Res.* 2012; 3(6):392-4.
- [9] Reta A, Gedefaw L, Sewunet T, Beyene G. Nasal carriage, risk factors and antimicrobial susceptibility pattern of methicillin resistant *Staphylococcus aureus* among school children in Ethiopia. *J Med Microb Diagn.* 2015;4(1):177.
- [10] Chatterjee SS, Ray P, Aggarwal A, Das A, Sharma M. A community-based study on nasal carriage of *Staphylococcus aureus*. *Indian J Med Res.* 2009;130(6):742-8.
- [11] Ceres P, Robert Dennis G, Shirley O. Staphylococcus aureus nasal carriage rates among children between oneto-five years in Barangay Pio Del Pilar, Makati City.2017; 24-33.
- [12] Pathak A, Marothi Y, Iyer R, Singh B, Sharma M, Eriksson B et al. Nasal Carriage and Antimicrobial susceptibility of *Staphylococcus aureus* in healthy preschool children in Ujjain, India. *BMC Pediatrics.* 2010;10(1).
- [13] Ramana K, Mohanty S, Wilson C. Staphylococcus aureus colonization of anterior nares of school going children. *Indian J Pediatr.* 2009;76(8):813-16.
- [14] Sanjib A, Sujan K, Ashish P, Anjana KC, Rajani M, Puspa K, et al. Nasal colonization of *Staphylococcus aureus* and their antibiograms among school children in Bharatpur, Nepal. *J Coll Med Sci-Nepal.* 2018;14(4):172-7.
- [15] Singh AK, Agarwal L, Kumar A, Sengupta C, Singh RP. Prevalence of nasal colonization of methicillin-resistant *Staphylococcus aureus* among school children of Barabanki district, Uttar Pradesh, India. *J Family Med Prim Care.* 2018;7:162-6.
- [16] Heckel M, Geißdorfer W, Herbst FA, Stiel S, Ostgathe C, Bogdan C. Nasal carriage of methicillin-resistant *Staphylococcus aureus* (MRSA) at a palliative care unit: A prospective single service analysis. *PLoS ONE.* 2017;12(12): e0188940.
- [17] Kulshrestha N, Ghatak T, Gupta P, Singh M, Agarwal J. Surveillance of health-care workers for nasal carriage to detect multidrug-resistant *Staphylococcus* spp. in a tertiary care center: An observational study. *Med J DY Patil Vidyapeeth.* 2019;12:39-43.
- [18] Eibach D, Nagel M, Hogan B, Azuure C, Krumkamp R, Dekker D, et al. Nasal Carriage of *Staphylococcus aureus* among Children in the Ashanti Region of Ghana. *PLoS ONE.* 2017;12(1): e0170320.doi:10.1371/journal.pone.0170320.
- [19] Koichi Y, Hiroki N, Hiroki F, Kiyotaka N, Etsuko T, Yasuyo O, et al. Clinical characteristics of methicillin-resistant coagulase negative staphylococcal bacteremia in a tertiary hospital. *Intern Med.* 2017;56:781-5.
- [20] ElSayed N, Ashour M, Amine AEK. Vancomycin resistance among *Staphylococcus aureus* isolates in a rural setting, Egypt. *GERMS* 2018;8(3):134-139. doi: 10.18683/germs.2018.1140.
- [21] Agarwal L, Singh A, Sengupta C, Agarwal A. Nasal carriage of Methicillin- and Mupirocin-resistant *S. aureus* among health care workers in a tertiary care hospital. *J Res Pharm Pract.* 2015;4(4): 182-6.
- [22] Venkatesh Bhavana, M., S. Joshi, R. Adhikary, and H. B. Beena. Mupirocin resistance in *Staphylococcus aureus* in a tertiary care hospital of south india - A prospective study. *Asian J Pharm Clin Res.* 2019;12(1):98-100.

Covid 19 Sentiment Analysis on Twitter Posts

Supreetha^{#1}, Mangala^{*2}

^{1,2}NMAMIT, Nitte

MCA Department, Nitte

¹supreethabhat8@gmail.com

^{2,*}mangalapshetty@nitte.edu.in

Abstract— social media is a source that generates huge amounts of data on an unprecedented scale. It is a platform for everyone to share their views, opinions and experience. It is not just a platform to provide information to the public, and also searches the public for information about the disease. Just as the emergence of Coronavirus (COVID-19) in 2019 is so surprising, it has fundamentally affected people around the world, and it is necessary to study the opinions of people about the COVID-19 pandemic. This project work focuses on the use of Twitter data for COVID-19 sentiment analysis. The analysis is based on machine learning algorithms. This article provides an analysis of people's reactions to the pandemic, their understanding of the disease and its symptoms, the preventive measures taken, and whether people are complying with the government guidelines. During the outbreak of the pandemic, postings on social media pages allowed health agencies and volunteers to better assess and understand the emotions and needs of the public in order to provide appropriate information and effective over.

Keywords—Covid 19, Corona Virus, Machine Learning

I. INTRODUCTION

Towards the end of 2019, the COVID-19, on-going Covid infection began in Wuhan, China. The infection has spread and conveyed locally in Wuhan and different spots in China, in spite of severe mediation measures and efforts executed around there. The World Health Organization proclaimed the Covid pandemic episode as a Global Public Health Emergency. Due to COVID-19, numerous human beings needed to lose their lives and its miles unexpected to recognise that the quantity of deaths related to COVID-19 stood a maximum danger to the world's public health. The main objective of the paper is to obtain a better understanding of the social opinions and views on COVID-19 and the way it has modified people's thinking over the past few months. Online media, for example, Twitter is chiefly helpful to separate data identified with the user's sentiments, evaluations and insights on a various number of points. Twitter is one of the quickest facts sharing platform amongst all online social networking media. Twitter is viewed as a smaller than normal contributing to a blog web-based media stage and it has an immense and developing number of clients each day. Messages or tweets on twitter variety from non-public facts to international information or events.

Examining this consistently generated records may be very interesting and informative allowing users or organizations to procure information. It facilitates the public position or relationship to understand how far broad society mindful about the turmoil flare-up, its signs and prudent steps. The tweets collected from twitter data for sentiment analysis of people on coronavirus using deep learning algorithms will help to study user's sentiments into three categories as positive, and negative during the disease outbreak.

II. LITERATURE SURVEY

A few specialists have been working on opinion investigation on various web-based media information especially on Twitter, not many fundamental commitments that assistance to find client perspectives or slants in different situations when pandemic occurring all throughout the planet. This segment covers some of the significant papers, which was utilized as reference. AD Dubey, A.D.[1], have accumulated the tweets more than 20 days (data assembled between 11th March and 31st March 2020) from 12 states to examine the blast of the novel Covid. The motivation behind this assessment is to acknowledge how people in those nations are reacting to illness epidemics. There's no vulnerability that, there some essential advances during the collection and execution of the functions, such as pre-processing and deleting extraneous data from the tweets. The results of these trials reveal that the majority of individuals in these civilizations think positively and are optimistic that things will improve, but it is also worth noting that there are symptoms of fear and melancholy. Nonetheless, four states particularly in Europe, believe they can't concur with the situation because of the flare-ups and pandemic over gigantic size of population. Alhaji et al.[2] use the Natural Language Toolkit (NLTK) module in Python to execute sentiment analysis on Arabic tweets using the Naive Bayes machine learning model. The gathered and analysed tweets containing hashtags related to seven government-imposed public health initiatives. Full scale tweets were explored in this assessment are 53,127. Except for one measure, the data reveal that there are more positive tweets than negative tweets. Ra, M. et al. [3] are dissected and envisioned, the impact of Covid (Coronavirus) on the world by using sentiment analysis algorithms and methods on the twitter dataset to comprehend

highly positive and very negative thoughts of the general population around the world. This uncovers that Naive Bayes AI approach has given better results and it's been believed to be the idea for essential learning. This additionally draws out another outfit strategy that utilizes slant score in light of the fact that the information work for the classifiers in AI, SVM, Max Entropy, Decision Tree, Boosting, and Random Forest. Accordingly, the LogitBoost, a mixed methodology, performed better with exactness of 74%. Prabhakar Kaila et al [4], used the Latent Dirichlet Allocation (LDA) approach on accumulated records to examine the Covid-19 outbreaks. The LDA procedures found the colossal related data on the COVID-19 contamination paramedic was negative conclusions such dread and positive notions like trust. Cherish Kay Pastor [5] uncover the estimation of the Filipinos in the impact of outrageous local area isolate brought about by COVID-19 Pandemic especially Luzon. The scientist likewise breaks down the impact of outrageous local area isolate and different impacts of the Pandemic to individual way of life dependent on the tweets of the clients. Natural Language Processing approach is use to decide the sentiments of clients from collected tweets. Feelings are managed as information for investigation. A subjective methodology was likewise utilized in deciding the impacts of the limit local area isolate in the Luzon region. Rajput [6] et. al. has analyzed the tweets distributed in January 2020. The tweets were examined for two primary aspects: first, understanding the word occurrence pattern, and then, second, sentiment recognition. Moreover, he expressed that the quantity of ids tweeting about the Covid has consistently increased, particularly in February and March. There were such countless rehashed words, for example, COVID-19, Covid, and Wuhan city. For the top thousand frequencies, N-grams models like unigram, bigram, and trigram repetition were created. Rajput inferred that nearly everyone observed some change rule which is very common appropriation. The figures and results were found very good. The remarkable boundaries were affected for the indistinguishable by -0.5266 for trigram, -1.273 for unigram, -1.375 for bigram. The graphs for the indistinguishable are represented. SSE, RMSE R2 are settled on integrity of the model. Medford et al. [7], used a set of COVID-19-related hashtags associated with COVID-19 to look for significant tweets throughout a two-week period from January 14 to 28th, 2020. Tweets are collected by Twitter API and put away as simple content. The frequency related key phrases are diagnosed and analysed which includes contamination prevention practices, vaccination, and racial prejudice. Following that, the sentiment evaluation is used to perceive every tweet's emotional valence such as negative, neutral or positive and essential emotions such as surprise, happiness, fear, disgust, joy or sadness. At last, an unsupervised machine learning algorithm is used to identify and analyse related topics in tweets over time. Kaur and Sharma [8] look at how individuals feel about coronavirus illness (COVID19), therefore they look at how various people feel about this condition. For this, the Twitter API was utilised to collect coronavirus-related tweets, which were then evaluated using machine learning methodologies and tools to determine positive, negative, and

neutral mood. Furthermore, the NLTK library is used to pre-process fetched tweets, and the Textblob dataset is used to analyse tweets. Finally, the intriguing results in positive, negative, and neutral emotions are displayed using various visualisations. Minchae Song, Hyunjung Park, Kyung-shik Shin [9] inspect the aftereffect of opinion examination highlights in finding ADR makes reference to strategies. Sentiment analysis reveals slightly advanced ADR qualifications in tweets and well-being-related forum postings, according to the findings. Even a state-of-the-art ADR recognition algorithm can be improved marginally by adding sentiment analysis elements, according to this study. Rahman, S. A. El, F. A. AlOtaibi, and W. A. AlShehri . [10] demonstrated that AD-related tweets used to sustain public disgrace, which affected negative assumptions for people with the sickness.

III. METHODOLOGY

A. Dataset

This study consolidated the information of Indian user tweets from the Twitter site during the COVID-19 shutdown period in-country. The data collection, which consists of 1,79,108 tweets, was retrieved from github.com (<https://github.com/gabrielpreda/CoViD-19-tweets> (accessed on 12 January 2021)) and contains cleaned tweets about COVID-19, coronavirus, lockdown, and other topics.

B. Tweets Cleaning

Now a days, twitter users use emojis along with alphanumeric characters to express their emotions. The tweets in their original format cannot be analysed. In this paper, neattext simple Natural Language Processing (NLP) package is used for cleaning textual data (removing hashtags, emojis, punctuations, spaces and urls).

C. Sentiment Analysis

Sentiment Analysis is fundamentally the way toward deciding the demeanor or the feelings of the user, that is weather positive or negative or neutral.

In this work, Python worked in bundle TextBlob is utilized to perform conclusion investigation of tweets relating to the Covid flare-up. The slant capacity of TextBlob returns two properties: polarity and subjectivity. Rule based methodology is utilized, where the guidelines are physically characterized to perform stemming and covering the content information into tokens, and afterward arranging the tokens in positive, neutral, and negative classes as indicated by the polarity.

Individual tweets' polarity values have been calculated. The following is how these values are interpreted: polarity greater than 0 infers positive; polarity less than 0 infers negative;

Covid 19 Sentiment Analysis on Twitter Posts

polarity equal to 0 infers neutral. The polarities range between -1 to 1. Subjectivity generally refers to personal opinion, emotion or judgement which lies in range of [0,1].

The table1 represents the count of positive, neutral and negative tweets based on the polarity and subjectivity of the tweets in the dataset.

The count of most common words from tweets text can be calculated by importing Counter class from Collection library. Counter method is applied to extract the most common words in positive sentiment, negative sentiment and neutral sentiment along with their count.

IV. RESULTS

In this section, the outcomes received from the sentiment evaluation of the twitter datasets is discussed. From Table1 we can observe that out of 1,79,108 tweets, the dataset has 1,336 more neutral sentiment tweets compared to the positive sentiment which is 74,154. We can examine that the negative sentiments are very less compared to the positive and negative sentiments.

TABLE 1 TWEETS CLASSIFICATION

Sentiment	Count
Positive	74154
Negative	29464
Neutral	75490

Figure 1 corresponds to the bar chart that is inferred from Table 1. The majority of the tweets are neutral sentiments followed by positive sentiment. Figure 2 represents the most common words with their count as scores. Figure 2.a represents the bar chart that displays the most common words in positive sentiment along with their score. It shows that the word ‘cases’ has highest frequency and ‘2020’ has the lowest frequency. From Figure 2.b we can see that the words in neutral sentiment such as help, need, health, mask etc has equal frequencies. Figure 2.c shows the bar chart of the most frequent words in negative sentiment tweets. Here, the word case has the highest score.

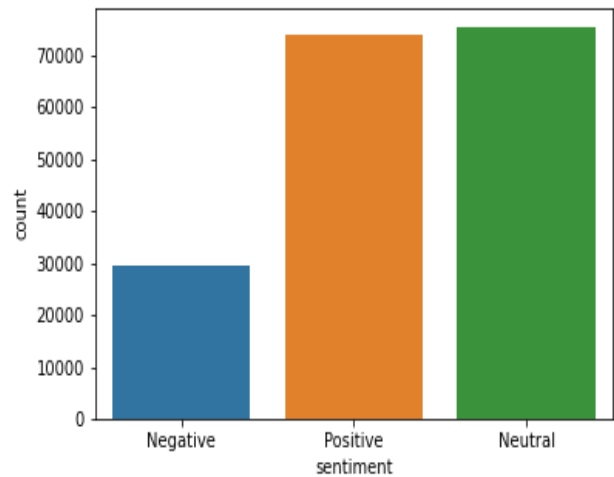


Fig. 1 Classification of Tweets

N.M.A.M. INSTITUTE OF TECHNOLOGY, NITTE – 574110

N.M.A.M. Institute of Technology was started in the year 1986, as a part of Nitte Education Trust, Mangalore, and celebrated its Silver Jubilee in 2011. The Institute is named in fond memory of Nitte Mahalinga Adyanthaya, a distinguished engineer of the district. From the year 2022, it is recognized as off campus center of Nitte (Deemed to be University), however, a few remaining batches of Engineering are still affiliated with the Visvesvaraya Technological University, Belagavi, as autonomous institutions and is recognized by the All India Council for Technical Education (AICTE), New Delhi.

Presently seven UG Programs are accredited by the National Board for Accreditation and the institution is certified to the ISO9001 – 2008 standards for quality education. The Institute is accredited With 'A' grade by NAAC. For supporting start-up companies, Atal Incubation Center is established at N.M.A.M.I.T., Nitte with a grant of 9 crores by NITI AAYOG, Government of India. The Institute has been awarded "E-LEAD: E-Learning Excellence for Academic Digitization" certification by QS I-GAUGE for the year 2020. This is in recognition of the college's technological capabilities in support of online learning.

The Institute offers B.E, M.Tech and Ph.D programs in various Engineering and Technology disciplines. The graduate programs comprised of 10 branches of Engineering – Artificial Intelligence & Machine Learning, Electronics & Communication Engineering, Computer Science & Engineering, Computer & Communication Engineering, Civil Engineering, Electrical & Electronics Engineering, Information Science & Engineering, Bio-Technology, Robotics & Artificial intelligence and Mechanical Engineering.

The Institute's postgraduate programs include, Master of Technology in 6 disciplines, Master of Computer Applications and Master of Business Administration. Besides these, students also pursue their M.Sc.(Eng.) and Doctoral Programs at the Institute. The Institute got an academic autonomy in the year 2007, bring much needed flexibility to innovate in terms of curriculum, education delivery and evaluation.

